

GraviDy: a GPU modular, parallel N -body integrator

Cristián Maureira-Fredes^{1, 2, *} and Pau Amaro-Seoane³

¹ Max Planck Institute for Gravitational Physics (Albert-Einstein-Institut), D-14476 Potsdam, Germany.

² Universidad Técnica Federico Santa María, Avenida España 1680, Valparaíso, Chile.

³ Institut de Ciències de l'Espai (CSIC-IEEC) at Campus UAB, Carrer de Can Magrans s/n 08193 Barcelona, Spain

Institute of Applied Mathematics, Academy of Mathematics and Systems Science, CAS, Beijing 100190, China

Kavli Institute for Astronomy and Astrophysics, Beijing 100871, China

Zentrum für Astronomie und Astrophysik, TU Berlin, Hardenbergstraße 36, 10623 Berlin, Germany

draft May 25, 2022

ABSTRACT

Context. A wide variety of outstanding problems in astrophysics involve the motion of a large number of particles ($N \gtrsim 10^6$) under the force of gravity. These include the global evolution of globular clusters, tidal disruptions of stars by a massive black hole, the formation of protoplanets and the detection of sources of gravitational radiation.

Aims. The direct-summation of N gravitational forces is a complex problem with no analytical solution and can only be tackled with approximations and numerical methods.

Methods. To this end, the Hermite scheme is a widely used integration method. With different numerical techniques and special-purpose hardware, it can be used to speed up the calculations. But these methods tend to be computationally slow and cumbersome to work with.

Results. Here we present a new GPU, direct-summation N -body integrator written from scratch and based on this scheme. This code has high modularity, allowing users to readily introduce new physics, it exploits available high-performance computing resources and will be maintained by public, regular updates.

Conclusions. The code can be used in parallel on multiple CPUs and GPUs, with a considerable speed-up benefit. The single GPU version runs about 200 times faster compared to the single CPU version. A test run using 4 GPUs in parallel shows a speed up factor of about 3 as compared to the single GPU version. The conception and design of this first release is aimed at users with access to traditional parallel CPU clusters or computational nodes with one or a few GPU cards.

Key words. N -body systems – Astrophysics – High Performance Computing

1. Motivation

The dynamical evolution of a dense stellar system such as e.g. a globular cluster or a galactic nucleus has been addressed extensively by a number of authors. For Newtonian systems consisting of more than two stars we must rely on numerical approaches which provide us with solutions that are more or less accurate. In this sense, one could make the following coarse categorisation of integration schemes for pure stellar dynamics: those which are particle-based and those which are not. In the latter, the system is treated as a continuum, so that while we know the general properties of the stellar system such as the mean stellar density, of the average velocity dispersion, we do not have information about specific orbits of stars. To this group, belongs direct integration of the Fokker-Planck equation (Inagaki & Wiyanto 1984; Kim et al. 1998) or moments of it (Amaro-Seoane et al. 2004; Schneider et al. 2011), including Monte Carlo approaches to the numerical integration of this equation (Spitzer & Hart 1971). A particle-based algorithm, however, assumes that a particle is tracing a star, or a group of them. In this group, the techniques go back to the early 40's and involved light bulbs (Holmberg 1941). The first computer simulations were performed at the Astronomisches Rechen Institut, in Heidelberg, Germany, by (von Hoerner 1960, 1963), using 16 and 25 particles. These first steps led to the modern N -body algorithms.

We can distinguish two types of N -body algorithms: the so-called collision-less, where a star just sees the background potential of the rest of the stellar system (e.g. the Barnes-Hut treecode or the fast multipole method Barnes & Hut 1986; Greendard 1987, which scale as $O(N \log N)$ and $O(N)$, with N the particle number, respectively), and the more expensive collisional one, or “direct-summation”, in which one integrates all gravitational forces for all stars to take into account the graininess of the potential and individual time steps, to avoid large numerical errors. This is important in situations in which close encounters between stars play a crucial role, such as in galactic nuclei and globular clusters, because of the exchange of energy and angular momentum. The price to pay however is that they typically scale as $O(N^2)$.

A very well known example is the family of direct-summation Nbody integrators of Aarseth (see e.g. Aarseth 1999; Spurzem 1999; Aarseth 2003)¹ or also KIRA (see Portegies Zwart et al. 2001a)². The progress in both software and hardware has reach a position in which we start to get closer and closer to simulate realistic systems.

However, the scaling $O(N^2)$ requires supercomputers, such as traditional Beowulf clusters, which requires a parallelisation of the code, such as the version of Nbody6 developed

¹ All versions of the code are publicly available at the URL <http://www.ast.cam.ac.uk/~sverre/web/pages/nbody.htm>

² <http://www.sns.ias.edu/~starlab/>

* Cristian.Maureira.Fredes@aei.mpg.de

by Spurzem and collaborators, N_{BODY}6++³ (Spurzem 1999), or special-purpose hardware, like the GRAPE (short for GRAVity PipE⁴) system. The principle behind GRAPE systems is to run on a special-purpose chip the most time consuming part of an N -body simulation: the calculation of the accelerations between the particles. The remainder is calculated on a normal computer which serves as host to the accelerator board(s) containing the special purpose chips. Such a system achieves similar or even higher speeds than implementations of the N -body problem on supercomputers (see e.g. Taiji et al. 1996; Makino & Taiji 1998; Makino 1998; Fukushima et al. 2005).

On the other hand, modern graphics processing units (GPUs) offer a very interesting alternative. They have been mostly used in game consoles, embedded systems and mobile phones. They were originally used to perform calculations related to 3D computer graphics. Nevertheless, due to their highly parallel structure and computational speed, they can very efficiently be used for complex algorithms. This involves dealing with the parallel computing architecture developed by NVIDIA⁵, the Compute Unified Device Architecture (CUDA). This is the main engine in NVIDIA GPUs, and it has been made accessible to developers via standard programming languages, such as C with NVIDIA extensions compiled thanks to a PathScale Open64 C compiler. This is what allows us to create binary modules to be run on the GPUs. Another option is Open Computing Language (OpenCL)⁶, which offers a framework to write parallel programmes for heterogeneous systems, including also computational nodes with field-programmable gate arrays (FPGAs), digital signal processors (DSPs), among others. CUDA, and also OpenCL are “the doors” to the native instruction set and memory of the parallel elements in the GPUs. This means that these can be handled as open architectures like CPUs with the enormous advantage of having a parallel-cores configuration. More remarkably, each core can run *thousands* of processes at the same time. We selected CUDA over OpenCL, because our systems are equipped with NVIDIA GPUs, even though we note that OpenCL has shown similar performance to CUDA in N -body simulations (Capuzzo-Dolcetta & Spera 2013).

There has been recently an effort at porting existing codes to this architecture, like e.g. the work of (Portegies Zwart et al. 2007; Hamada & Iitaka 2007; Belleman et al. 2008) on single nodes or using large GPU clusters (Berczik et al. 2011; Nitadori & Aarseth 2012; Capuzzo-Dolcetta et al. 2013) and recently, the work by (Berczik et al. 2013) using up to 700 thousand GPU cores for a few million bodies simulation with the ϕ -GPU⁷ code, which reached in their work about the half of the peak of the new Nvidia Kepler K20 cards.

Large-scale (meaning number of particles) simulations have recently seen an important improvement with the work of Wang et al. (2015, 2016). In his more recent work of 2016, Wang and collaborators integrated systems of one million bodies in a globular cluster simulation, using from 2,000 to 8,600 hours of computing time.⁸

In this paper we present the initial version of GRAVIDY (Gravitational dynamics), a highly-modular, direct-summation N -body code written from scratch using GPU technology ready

to integrate a pure dynamical gravitational system. In section 2 we present in detail the structure of the code, the most relevant and innovative parts of the algorithm, and their implementation of the scheme in the idiom of GPU computing. In section 3 we check our code with a series of well-known tests of stellar dynamics for a dense stellar system and evaluate global dynamical quantities and we also evaluate the performance of the GPU version against the CPU one. In section 5 we summarise our work and give a short description of the immediate goals that will be described in upcoming publications.

We have decided to focus on single-node clusters (meaning one or more GPU cards embedded in a host PC) and traditional multi-CPU clusters (e.g. Beowulf clusters), since this setup is more common to most users who aim to run middle-scale simulations. In the appendices we give a succinct description on how to download the code, how to compile it, and the structure of the data. Additionally, we describe the usage of a set of python tools to analyse the results. Moreover, we also introduce a simple visualisation tool based on OpenGL, which can provide us with information sometimes difficult to obtain with two-dimensional graphics. In particular, we have made a significant effort in documentation and modularity, since it is our wish that the code is used, shaped and modified at will.

2. The current algorithm

2.1. The integration scheme

In this section we give a very brief introduction to the numerical N -body problem. We refer the reader to e.g. (Aarseth 2003; Heggie & Hut 2003) or the excellent on-line course “The art of computational science”⁹. The evolution of an N -body system is described by the second order ordinary differential equation

$$\ddot{\mathbf{r}}_i = -G \sum_{\substack{j=1 \\ j \neq i}}^N m_j \frac{(\mathbf{r}_i - \mathbf{r}_j)}{|\mathbf{r}_i - \mathbf{r}_j|^3}, \quad (1)$$

where G is the gravitational constant, m_j is the mass of the j th particle and \mathbf{r}_j the position. We denote vectors with bold fonts. The basis of the problem is purely dynamical, because the orbital evolution is determined exclusive by the gravitational interaction.

The total energy of the system is a useful quantity to keep track of every time step in the integration. It is given by the expression

$$E = \frac{1}{2} \sum_{i=1}^N m_i \mathbf{v}_i^2 - \sum_{i=1}^N \sum_{j>i}^N \frac{G m_i m_j}{|\mathbf{r}_i - \mathbf{r}_j|}, \quad (2)$$

where \mathbf{v}_i is the velocity of the particle i .

To numerically integrate the system of equations we adopt the 4th-order Hermite integrator (H4 from now onwards) presented in (Makino 1991; Makino & Aarseth 1992) (and see also Aarseth 1999, 2003). H4 is a scheme based on a predictor-corrector scenario, which means that we use an extrapolation of the equations of motion to get a predicted position and velocity at some specific time. We then use this information to get the new accelerations of the particles, later we correct for the predicted values using interpolation based on finite differences terms. One

⁹ <http://www.artcompsci.org/>

³ Available at this URL <http://silkroad.bao.ac.cn/nb6mpi>

⁴ <http://grape.c.u-tokyo.ac.jp/grape>

⁵ <http://www.nvidia.com>

⁶ <https://www.khronos.org/opencl/>

⁷ <ftp://ftp.mao.kiev.ua/pub/berczik/phi-GPU/>

⁸ This impressive achievement was rewarded with a bottle of Scotch whisky (not whiskey), kindly and generously offered to him by Douglas Heggie during the excellent MODEST 15-S in Kobe.

can use polynomial adjustment in the gravitational forces evolution among the time because the force acting over each particle changes smoothly (which is the reason why adding a very massive particle representing e.g. a supermassive black hole will give you sometimes a headache). To advance the system to the following integration time we approximate the equations of motion with an explicit polynomial. This prediction is less accurate, but it is improved in the corrector phase, which consist of an implicit polynomial that will require good initial values to scale to a good convergence.

This is a fourth-order algorithm in the sense that the predictor includes the contributions of the third-order polynomial, and after deriving the accelerations, adds a fourth-order corrector term. In the remaining of this paper we focus on the implementation of the scheme into our GPU (and CPU) code and how to maximise all of the HPC resources available. For a detailed description of the idea behind H4, we refer the reader to the article in which it was presented for the first time, (Makino & Aarseth 1992).

An advantage of the choice for H4 is that we can use the family of Aarseth’s codes (among others) as a test-bed for our implementation. These codes –some of which adopt H4, but not all of them– have been in development for more than 50 years. The codes are public and have been widely used and validated, improved and checked a number of times by different people, they have been compared to other codes and even observational data. In this regard, to test our implementation and parallelisation of H4, the access to the sources of the codes is an asset.

2.2. Numerical strategy

A main goal in the development of GRAVIDY is its *legibility*. We have focused in making it easy to read and modify by other users or potential future developers without compromising the computational performance of the algorithm. This means that we have made a significant effort in keeping a clear structure in the source code so that, in principle, it can be well understood by somebody who has not previously worked with it with relatively little effort. The modularity of the code should allow new users to easily implement new physics or features into it or adapt it to the purposes they seek. It is unfortunately easy –at least to a certain extent– to miss either clarity in coding or performance, when trying to have both in a code. For instance, if we want to obtain the best performance possible, one has to use low-level instructions that for an outside user might result into something difficult to understand when reading or trying to modify the source code. On the other hand, name conventions for files, functions and variables might become a burden to certain applications.

While most existing N -body codes have achieved certain balance between the two to some degree, it is difficult to adapt them to new architectures and technology to boost their performance. For the development of GRAVIDY, we have followed the next steps:

Serial implementation: The first logical step in developing a code using GPU technology is –in our opinion– to have a full, one-thread CPU version. This allows us to check for the robustness of the code, as it is usually easier to find and fix any potential bugs when introducing new features or improving the performance.

Profiling and assessment: After that, we localise the main bottlenecks of the code. One obvious one is the computation of the gravitational forces, but it is in general a good idea to

Listing 1. `gprof` output of a serial GRAVIDY simulation, using 1024 particles up to 1 N -body time unit, showing the amount of time of the particle-particle force interaction. Some output columns are omitted.

```
Flat profile:
Each sample counts as 0.01 seconds.
%   self   time   seconds  calls name
92.5  12.05 125186180 Hermite4::force_calculation(...)
 1.1   0.15   5161 Hermite4::predicted_pos_vel(...)
 0.3   0.04   5161 Hermite4::correction_pos_vel(...)
 0.2   0.03   5161 Hermite4::next_integration_time(...)
 0.2   0.03   5161 Hermite4::find_particles_to_move(...)
 0.0   0.00   5161 Hermite4::update_acc_jrk(...)
...
```

check for other potential hindrances. For this, we typically employ `gprof`¹⁰.

In the case of our CPU code, for instance, we see that more than 93% of the CPU time goes into the updating of a particular function, the gravitational interaction, as displayed in listing 1. There are some tools to perform the profiling of CUDA application, but they are not discussed in this work. The idea of keeping an updated CPU version of the code, helps to find potential errors or bottlenecks of the parallel version.

Granularity and hot-spots: After having identified the bottlenecks of the code, the objective is to use HPC to attack them to speed up the calculations. Ideally, this would be a one-time task, but the fact is that the implementation, which will be described in detail later, depends on the hardware at our disposal, which keeps quickly evolving in the case of GPU technology, the release of new libraries and new ideas to speed up the force calculation. This means that the code is on a cycle process of constant improvement, and has to be revisited regularly.

Before we get into the details of the parallelisation, it is important to introduce the concept of *granularity*. This is a classification of the algorithm at play based on the communication and performance. We usually distinguish two types of granularity: *fine-grained* algorithms are computationally lightweight, because the task performed (in this case by threads) is small compared with communication, which is a frequent process. On the other hand, *coarse-grained* algorithms do the opposite. They require less communication but are computationally more demanding for each task.

A good example of the difference in granularity is the comparison of Message Passing Interface (MPI) and GPU computing: usually, a code relying on MPI splits a bigger task in many sub-tasks, which are sent to different computational nodes. After finishing the computation, the data are gathered in a so-called “master” node. Programming in GPU is quite different; there is a frequent communication between the CPU and the GPU and the tasks assigned to the many threads available in the GPUs are quite small. This is why in GPU computing, the finer the granularity, the more efficiently we can follow a parallelisation scheme.

Optimisation: In the process of parallelisation of a code in CUDA one has to bear in mind the following characteristics, inherent to this programming language and GPU architecture: (i) while the use of local memories improves the

¹⁰ GNU Gprof Documentation: <http://www.cs.utah.edu/dept/old/texinfo/as/gprof.html>

performance of a CUDA code, the global memory (off-chip memory) is accessed in “chunks”, multiples of 32 bytes, the so-called *warps*. Failing to use them completely leads to a so-called *memory coalescing*; i.e. a waste of bandwidth. (ii) Indeed, the usage of shared memory can lead to a number of issues if not employed properly: since we are accessing chunks of memories in warps, we *have* to retrieve information from the global memory also in chunks. Moreover, if threads within a warp access different banks of memory, we will confront a *bank conflict*. E.g. two threads access the same value from the local memory. (iii) *Divergence* is another issue to take into account. When a control flow statement (e.g. if-else) is inside a kernel execution and it splits the threads to perform different pieces of code, the problem is that one of those tasks could be more expensive computationally. Hence, at the moment of synchronisation, the threads executing the less expensive code will need to wait for the others to achieve a synchronisation. While it is not forbidden to use control flow, we need to at least leave one warp do some task. This means that control flow must be at warp level; different warps can do different tasks without running into divergence. (iv) The hardware that we have at our disposal plays a crucial role: GPU chips are formed by several Streaming Multiprocessor (SM), which contain the GPU cores (Streaming Processor, SP). All SM can execute only one warp per core at a time, so that we must try to use them constantly, which is what we refer to as the *occupancy*. This will be determined by the usage of every thread in a block respect to the registers and the shared memory, which is GPU-dependent.

2.3. Particular choices

Object oriented programming: Object oriented programming (OOP) is a powerful paradigm that allows us to program an algorithm as objects interactions. In GRAVIDY, we use OOP. The reason beneath it is related to our parallelisation scheme, which is described below, more concretely with the data structure we have chosen.

We have mainly two possible choices for data structures: classes with arrays, or Arrays of Objects, which follows the basic idea of Struct of Arrays (SoA) and Array of Structs (AoS). For GRAVIDY we have chosen *classes* with arrays for the main units of the program structure. It is a good strategy to minimise the data transfer between Host and Device, so as to avoid having large communication times.

Calling the GPU kernels¹¹, we only transfer a piece of information relative to all the bodies, e.g. only the masses of the bodies or only the position of a certain amount of bodies, but not all of them. Because of this, we deem it more practical to handle the data transfer of our scheme by using arrays containing information on different particles.

In practice, this means that we use the GPU to only compute some specific integration steps like the force calculation, and the energy. Hence, we have to transfer to the GPU at every iteration the predicted positions and velocities, to then transfer from the GPU the new calculated forces (i.e. the acceleration and its first derivative). It is also possible to have all the integration steps on the GPU, but we do not see a significant improvement for our integrator scheme. Higher integration

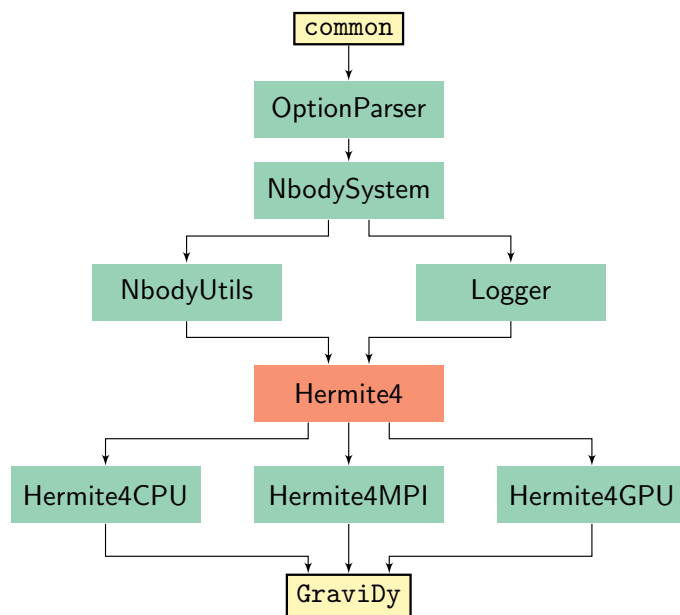


Fig. 1. Class diagram of the code that shows the hierarchy of the application structure (GRAVIDY).

schemes show a better performance using the whole process on the GPU (Capuzzo-Dolcetta et al. 2013)

It is not required to update the forces of all the particles, so that we encapsulate the information of the active particles, and then we transfer the AoS to the GPU. All the remaining attributes of the bodies (i.e. those not transferred to the GPU) are just class-members (arrays), and need to be in the host CPU. An example of this could be large linear arrays, such as the time steps of the particle.

Class distribution: Since our code is using OOP, we describe a brief interaction between the classes in Fig. 1. The main header, `common.hpp`, contains the definition of the constants, structures, macros, etc. The idea behind this model is to easily be able to add more features in upcoming versions of our code, from new utilities functions to new integration schemes.

Every class is in charge of a different mechanism, from getting the integration options from command-line, to the different integration methods using parallelism or not¹².

Double-precision (DP) over Single-precision (SP): Using DP or SP in N -body codes has been already addressed by different authors in the related literature (see e.g. Hamada & Iitaka 2007; Nitadori 2009; Gaburov et al. 2009). Using DP is not the best scenario for GPU computing, because there is a decrease factor in the maximum performance that a code can reach. We can reach only half of the theoretical maximum performance peak, which depends on each individual card: for example, the NVIDIA Tesla C2050/M2050 has a peak of the processing power in GFLOPs 1030.46 with SP, but only 515.2 with DP. We choose to use DP for a more accurate numerical resolution, but note that one of the goals of the next versions of our code it is to try different mixed-precision approach, (Aarseth 1985), or try pseudo DP (Nitadori 2009), which is currently used in the code ϕ -GPU (Berczik et al. 2011).

¹¹ We depict as “kernel” the set of functions which can be executed on the GPU

¹² For more information, please refer to the code documentation

2.4. The implementation scheme

These are the steps that GRAVIDY follows when running a simulation:

1. Memory allocation of the CPU and GPU arrays.
2. Initialisation of the variables related to the integration, like the integration time.
3. Copy the initial values of positions, velocities and masses of the particles to the GPU to calculate the initial system energy, and calculate the initial acceleration and its first derivative, the so-called “jerk”. The cost of this force calculation is $O(N^2)$.
4. Copy the initial forces from the GPU to CPU.
5. Find the particles to move in the current integration time, N_{act} , with a cost $O(N)$.
6. Save the current values of the forces, to use them in the correction step, with a cost $O(N)$.
7. Integration step:
 - (a) Predict the particle’s positions and velocity up to the current integration time, with cost $O(N)$.
 - (b) Copy of the predicted positions and velocities of all the particles from the CPU to the GPU.
 - (c) Update the N_{act} particles on the GPU, which is explained in detail in section 2.5.
 - i. Copy the N_{act} particles to a temporary array on the GPU.
 - ii. Calculate the forces between the particles on the GPU, with a cost $O(N_{\text{act}} \cdot N)$.
 - iii. Reduce forces on the GPU.
 - iv. Copy the new forces from the GPU to the CPU.
 - (d) Correct the position and velocity of the N_{act} updated particles on the CPU, $O(N_{\text{act}})$.
 - (e) Copy the positions and velocities of the corrected N_{act} particles from the CPU to the GPU.

GRAVIDY adheres to the usual good practise of every N -body code with softening:

- *Direct-summation*, also known as particle-particle strategy, This approach is the simplest way to address the task of calculating the exerted force by all the $N - 1$ bodies on a single body that we need to update at certain timestep. This brute-force procedure has an order $O(N^2)$, which represents the bottleneck of the algorithm.
- *Softened point-mass potential*, all particles are represented by a dimensionless point mass. We introduce a softening parameter (ϵ) in the distance calculation between two bodies while we get the new forces,

$$\ddot{\mathbf{r}}_i = -G \sum_{\substack{j=1 \\ j \neq i}}^N \frac{m_j}{(r_{ij}^2 + \epsilon^2)^{3/2}} \mathbf{r}_{ij}, \quad (3)$$

so as to handle the situation in which two bodies get closer.

- *Block time steps*, It is not straightforward to have an N -body code using individual time steps in parallel computing, because the idea behind massive parallelism is to perform the same task on different data chunks. We use the block time steps algorithm (Press 1986), to update group particles simultaneously. This scheme has been adopted by a number of authors (Portegies Zwart et al. 2001b; Hut 2003; Aarseth 1999, 2003; Harfst et al. 2008; Nitadori & Aarseth 2012). The main idea is to have several blocks (groups) of particles sharing the same time steps. This decreases the amount of

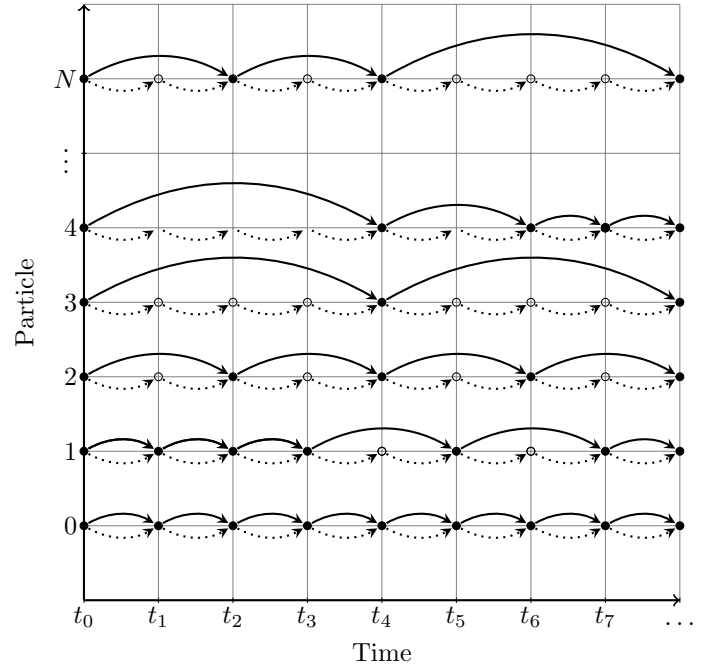


Fig. 2. Block timesteps illustration. The different blocks are represented by the length of the jump. Each particle is predicted (but not moved) at every time t (dotted arrows), even if it is not the turn of their block timestep (empty circles). The particles will be updated (and moved) only in their corresponding block timestep (filled circles). Whenever a particle is updated, its block timestep can be change. In this illustration, particles 1, 4 and N change their block (length of the jump).

operations of the integration process, which allows us to obtain a similar accuracy to the individual time steps scheme. In this scenario the parallelisation is ideal, because compared with the individual scheme, we have several chunks of threads working on different blocks of particles. In this approach, particle i is part of the lower n th block time step between two quantities,

$$2^n \Delta t_s \leq \Delta t_i < 2^{n+1} \Delta t_s. \quad (4)$$

Δt_i is determined by equation 21, and Δt_s is a constant. The particles distribution among the different blocks is determined by the following condition,

$$\Delta t_{i,\text{new}} = 2^{\lceil \log_2 \Delta t_i \rceil - 1}, \quad (5)$$

and is described in Fig. 2.

For the boundaries of the timesteps, we use the Aarseth criterion (Aarseth 2003) for the lower limit of the timesteps allowed in the system:

$$\Delta t_{\min} = 0.04 \left(\frac{\eta_l}{0.2} \right)^{1/2} \left(\frac{R_{\text{cl}}^3}{\bar{m}} \right)^{1/2}, \quad (6)$$

where η_l is the initial parameter for accuracy, typically 0.01; R_{cl}^3 is the close encounter distance and \bar{m} the mean mass.

Usually $\Delta t_{\min} = 2^{-23}$. On the other hand, we set a maximum time step $\Delta t_{\max} = 2^{-3}$. When updating a particle’s timestep, if it is out the this boundaries, we modify the value to Δt_{\min} if $\Delta t < \Delta t_{\min}$, and to Δt_{\max} if $\Delta t > \Delta t_{\max}$.

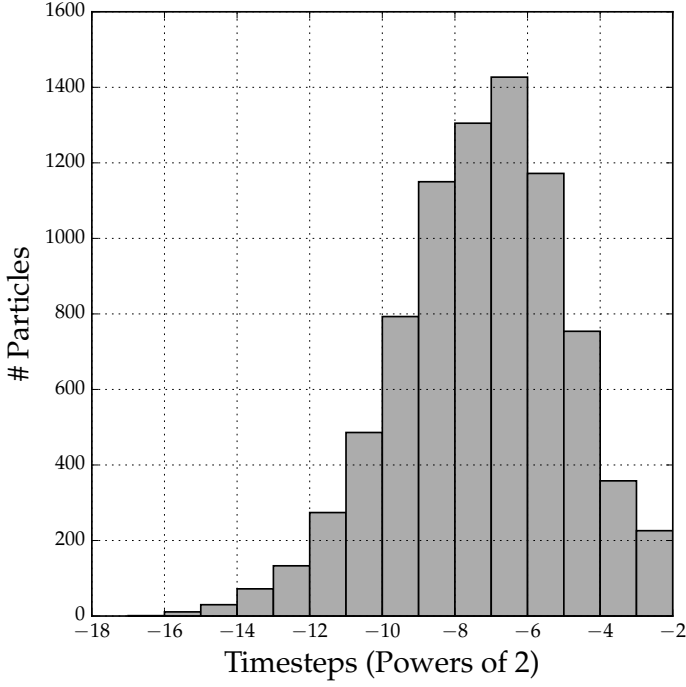


Fig. 3. Initial timesteps distribution of a Plummer system with $N = 8192$ particles, sampled in different groups (powers of 2). The numerical constraints of this powers of 2 are $[-23, -3]$.

The algorithm uses a Hermite of 4th order to integrate the evolution, which follows these steps:

1. Select the particles with the minimum $t_{i,0} + \Delta t_{i,0}$ and assign this minimum time to the global integration time t .
2. Calculate the predicted position ($\mathbf{r}_{i,\text{pred}}$) and velocity ($\mathbf{v}_{i,\text{pred}}$) at time t , for all i particles, using these expression:

$$\mathbf{r}_{i,\text{pred}} = \mathbf{r}_{i,0} + \mathbf{v}_{i,0}\Delta t_i + \frac{1}{2!}\mathbf{a}_{i,0}\Delta t_i^2 + \frac{1}{3!}\dot{\mathbf{a}}_{i,0}\Delta t_i^3 \quad (7)$$

$$\mathbf{v}_{i,\text{pred}} = \mathbf{v}_{i,0} + \mathbf{a}_{i,0}\Delta t_i + \frac{1}{2!}\dot{\mathbf{a}}_{i,0}\Delta t_i^2 \quad (8)$$

in this case, the $\Delta t_{i,0}$ is calculated as follows:

$$\Delta t_i = t - t_{i,0} \quad (9)$$

3. Calculate the acceleration ($\mathbf{a}_{i,1}$) and the jerk ($\dot{\mathbf{a}}_{i,1}$) using the predicted position and velocity only for the i -particles in which the global time t , is equal to $t_{i,0} + \Delta t_{i,0}$ ¹³.

$$\mathbf{a}_{i,1} = \sum_{\substack{j=0 \\ j \neq i}}^N Gm_j \frac{\mathbf{r}_{ij}}{(r_{ij}^2 + \epsilon^2)^{\frac{3}{2}}}, \quad (10)$$

$$\dot{\mathbf{a}}_{i,1} = \sum_{\substack{j=0 \\ j \neq i}}^N Gm_j \left[\frac{\mathbf{v}_{ij}}{(r_{ij}^2 + \epsilon^2)^{\frac{3}{2}}} - \frac{3(\mathbf{v}_{ij} \cdot \mathbf{r}_{ij})\mathbf{r}_{ij}}{(r_{ij}^2 + \epsilon^2)^{\frac{5}{2}}} \right], \quad (11)$$

where

¹³ Eq.(2) of Makino & Aarseth (1992) has a typo in the sign of the second term in the sum of $\dot{\mathbf{a}}_{i,1}$.

$$\mathbf{r}_{ij} = \mathbf{r}_{j,\text{pred}} - \mathbf{r}_{i,\text{pred}}, \quad (12)$$

$$\mathbf{v}_{ij} = \mathbf{v}_{j,\text{pred}} - \mathbf{v}_{i,\text{pred}}, \quad (13)$$

$$r_{ij} = |\mathbf{r}_{ij}| \quad (14)$$

It is important to note, that $(\mathbf{v}_{ij} \cdot \mathbf{r}_{ij})$ correspond to the *dot product*, and not a simple multiplication.

4. Calculate the 2nd and the 3rd derivative of the acceleration ($\mathbf{a}_{i,1}^{(2)}, \mathbf{a}_{i,1}^{(3)}$) using the third-order Hermite interpolation polynomial constructed using $\mathbf{a}_{i,0}$ and $\dot{\mathbf{a}}_{i,0}$:

$$\mathbf{a}_{i,1}(t) = \mathbf{a}_{i,0} + \dot{\mathbf{a}}_{i,0}\Delta t_{i,0} + \frac{1}{2}\Delta t_{i,0}^2 \mathbf{a}_{i,0}^{(2)} + \frac{1}{6}\Delta t_{i,0}^3 \mathbf{a}_{i,0}^{(3)} \quad (15)$$

where $\mathbf{a}_{i,0}$ and $\dot{\mathbf{a}}_{i,0}$ are the acceleration and jerk calculated at the previous time t , the second and third acceleration derivatives $\mathbf{a}_i^{(2)}$ and $\mathbf{a}_i^{(3)}$ are given by:

$$\mathbf{a}_{i,0}^{(2)} = \frac{-6(\mathbf{a}_{i,0} - \mathbf{a}_{i,1}) - \Delta t_{i,0}(4\dot{\mathbf{a}}_{i,0} + 2\dot{\mathbf{a}}_{i,1})}{\Delta t_{i,0}^2} \quad (16)$$

$$\mathbf{a}_{i,0}^{(3)} = \frac{-12(\mathbf{a}_{i,0} - \mathbf{a}_{i,1}) - 6\Delta t_{i,0}(\dot{\mathbf{a}}_{i,0} + \dot{\mathbf{a}}_{i,1})}{\Delta t_{i,0}^3} \quad (17)$$

where $\mathbf{a}_{i,1}$ and $\dot{\mathbf{a}}_{i,1}$ are the acceleration and the jerk at the time $t_i + \Delta t_i$.

5. After the previous calculation, it is necessary to add the corrections to the position and the velocity for the particle i at the time $t_i + \Delta t_i$

$$\mathbf{r}_{i,1} = \mathbf{r}_{i,\text{pred}} + \frac{1}{24}\Delta t_i^4 \mathbf{a}_{i,0}^{(2)} + \frac{1}{120}\Delta t_i^5 \mathbf{a}_{i,0}^{(3)} \quad (18)$$

$$\mathbf{v}_{i,1} = \mathbf{v}_{i,\text{pred}} + \frac{1}{4}\Delta t_i^3 \mathbf{a}_{i,0}^{(2)} + \frac{1}{24}\Delta t_i^4 \mathbf{a}_{i,0}^{(3)} \quad (19)$$

6. We then need to calculate the next timestep for the i particle ($\Delta t_{i,1}$) and time t using the following formulae:

$$t_{i,1} = t_{i,0} + \Delta t_{i,0} \quad (20)$$

$$\Delta t_{i,1} = \sqrt{\eta \frac{|\mathbf{a}_{i,1}||\mathbf{a}_{i,1}^{(2)}| + |\mathbf{j}_{i,1}|^2}{|\mathbf{j}_{i,1}||\mathbf{a}_{i,1}^{(3)}| + |\mathbf{a}_{i,1}^{(2)}|^2}}. \quad (21)$$

Here η is the accuracy control parameter, $\mathbf{a}_{i,1}$ and $\dot{\mathbf{a}}_{i,1}$ are already known, $\mathbf{a}_{i,1}^{(3)}$ has the same value as $\mathbf{a}_{i,0}^{(3)}$ due the third-order interpolation, and $\mathbf{a}_{i,1}^{(2)}$ is given by:

$$\mathbf{a}_{i,1}^{(2)} = \mathbf{a}_{i,0}^{(2)} + \Delta t_i \mathbf{a}_{i,0}^{(3)} \quad (22)$$

We depict the process of the integration in Figure 4.

2.5. The parallelisation scheme

As we have already mentioned, the bottleneck of any N -body code is the force calculation 4. In this respect, GRAVIDY is not different and a quick performance test to get the profile of our serial code yields almost 100% of the execution time in this calculation 1. We hence introduce a parallelisation scheme, which we discuss in detail now.

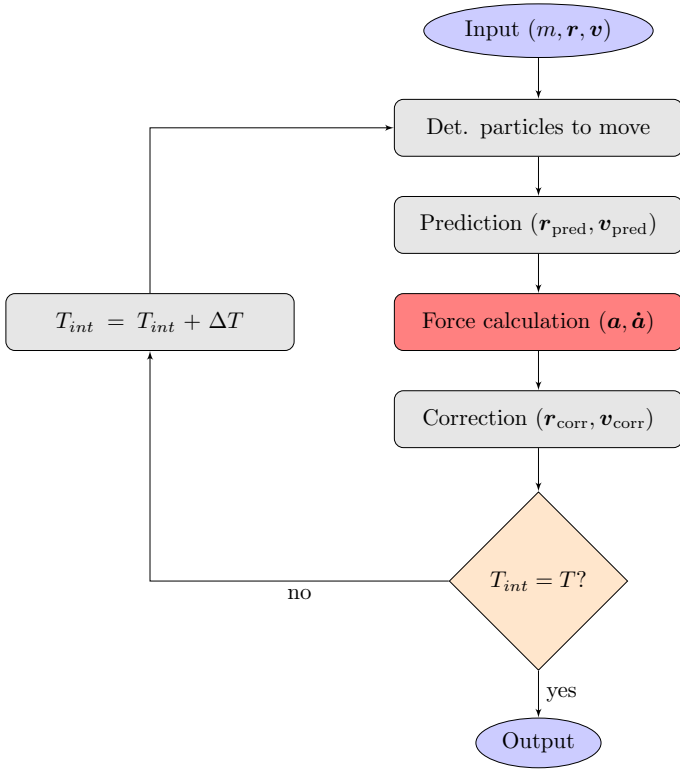


Fig. 4. Hermite integration scheme illustration. This flow diagram shows the steps of every iteration. The force calculation is marked with red, because it is the bottleneck of the computational time.

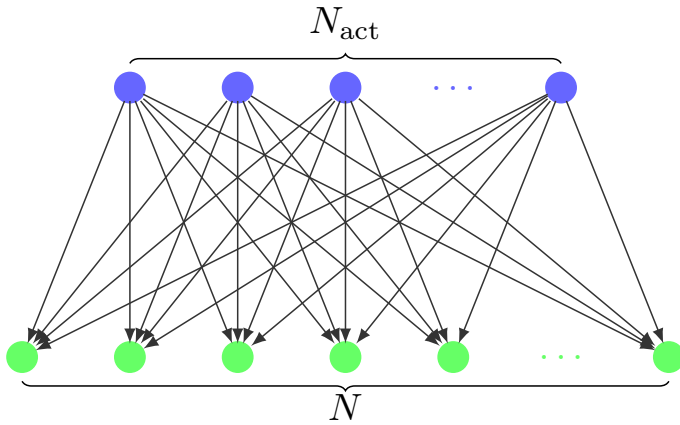


Fig. 5. Relation between the particles which will be updated in a certain integration time (N_{act}) and the whole set of particles (N). The relation between the active particles and the others is $N_{\text{act}} \ll N$ in non-synchronisation times.

GRAVIDy is based on a direct-summation Hermite 4th order integrator and uses block timesteps, so that in the force update process we have a nested loop for every i -active particle (which we will refer to from now with the subscript “act”). This means that for every particle which needs to be updated we have a loop run on the whole set of particles of our system to check whether particle j - is interacting with i -.

The whole process scales with the amount of i -particles, as we can see in Figure 5.

We then need to parallelise the loop corresponding to each of the i -particles. For each of them we circulate through all of

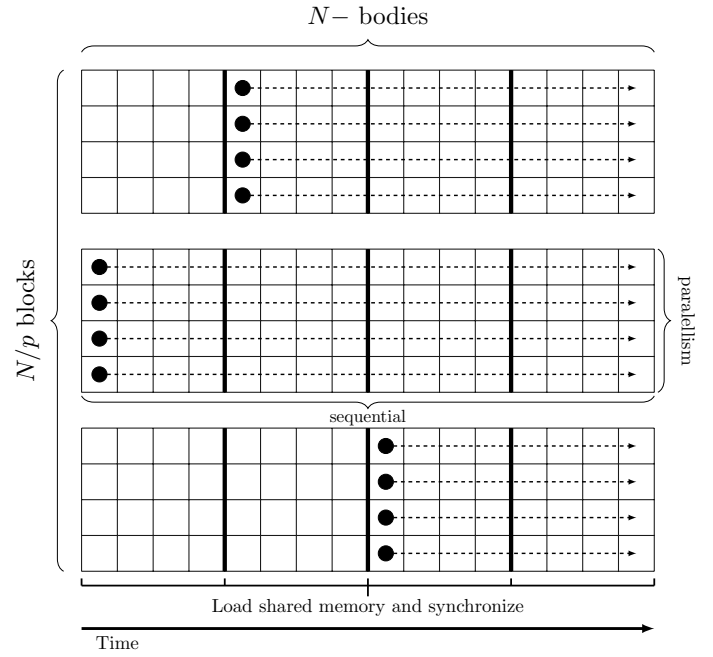


Fig. 6. Grid configuration using the *tiles* approach (This figure is based on GPU-Gems3 book (Nguyen 2007))

the j -particles, and this is the process which needs to be parallelised. Although this is in principle a straightforward scheme, since we focus on GPUs, we run into the following issues:

1. A GPU can launch a large number of threads, easily up to thousands of them. In our scenario, however, the number of active particles N_{act} is very small compared to the total amount of particles (N). This has an impact on the performance: we do not use all available threads, we are integrating a grid of $N_{\text{act}} \times N$ forces. When the number of active particles is very low our *occupancy* will be bad.
2. Contrary, in the case in which we have to move all particles, we will have an $O(N^2)$ parallelism, which maximises the GPU power. In this case, however, the *memory bandwidth* is the limitation factor, since every particle requires all information about all other $N - 1$ particles.

The $N \times N$ forces grid allows us to use *tiles*, as explained in Nguyen (2007), and introduced in a direct-summation N -body for the first time by Nitadori (2009). Using tiles means that we work with a square of the GPU grid of p rows and p columns, as depicted in Fig. (6). Instead of having the usual p^2 power that arises from all particles interacting with all particles, we need to only take into account the sum of p blocks in the shared memory of the GPU. Synchronisation only takes place at some particular moments, displayed as bold vertical lines in the figure, and we only have a load from global to shared memory of p particles per tile, which implies a reusing of existing information instead of loading new one. The circles in the figure represent that, given a certain moment, the calculation can be in any column, because the threads are synchronised during the computation. We evaluate the interactions row by row and have parallelism in every column.

Whilst tiles is optimal when we need to evaluate force interaction for all particles in the system, GRAVIDy rarely deals with this situation due to the nature of the base algorithms and main goals behind it. The amount of particles that we need to update

at every step is $N_{\text{act}} \ll N$, with N the total number of them. This means that we will be wasting computational resources, since some threads will not do the entire work. This is why we have to look for an alternative scheme which handles better the fact that we only need to move a subgroup of particles instead of the whole system.

It is better to have all particles handled by the GPU, and not only the active ones, because even though this subgroup is smaller, or even much smaller, it is more efficient from the point of view of the GPU, since the *occupancy* is improved. The parallelisation happens at j -level (i.e. when calculating the forces between active particles with the rest of the system). This idea was first implemented by Nitadori (2009), and has proven to yield very good performance.

The main ideas behind the j -parallelisation is how force calculation is done and the summation of the forces (“reduction” in HPC jargon):

- *Force calculation*: The interaction between the i -particle and the rest of the system is distributed among the GPU threads, which means that we launch N threads, and each of them calculates its contribution with the i -particle. After this calculation, we have an array with the contributions of each of the total number of particles, N . This corresponds to the upper part of Fig.(7), which illustrates a set-up of two GPUs. After the force calculation we end up with an array containing the information about the forces for all particles.
- *Force reduction*: In the lower part of the same Fig. we depict the summation of all of these forces, which is also performed in parallel, so that we use the blocks distribution of the GPU for this task.

So as to illustrate these steps, we give a particular example of a system with 1024 particles: let us assume that we need to move 300 of them ($N_{\text{act}} = 300$) at the moment of launching the kernel. Before this, we need to set up the kernel configuration. We define the grid size (number of thread blocks), and the block size (number of threads per block). These sizes are 3-component vectors, to help an easy identification of the *thread-ID* and *block-ID* at every kernel launch.

Since we have a two-phase force calculation process, we use a different configuration for each kernel call (block and grid size): one for the preliminary force calculation, which calculates the total force on an active particle, in 16 values (the JPBLOCK size), and another one to reduce those sets into the final total force on an active particle. We base our configuration on the idea presented in Nitadori & Aarseth (2012), with some variations of the data scheme. We use two-dimensional blocks to handle the indexes of the threads. In the case of the force calculation, we have:

```
1 dim3 blockSize(BSIZE, 1, 1); // (64, 1, 1)
2 dim3 gridSize(1 + Nact/BSIZE, JPBLOCKS, 1); // (5, 16, 1)
```

Firstly, we define the block size to 64. Next, we configure the grid: the first dimensions of the blocks (blockIdx.x = 5) are thought to handle the $N_{\text{act}} = 300$ particles (5 blocks \times 64 threads = 300 threads), and the second dimension of the blocks (blockIdx.y) JPBLOCKS, to handle the N particles in groups of $N/\text{JPBLOCK} = 64$. Lastly, we need 64 more threads to use the JPBLOCKS, which is the reason for having the 1+ at the beginning of the first dimension of the grid. After this process, the temporary forces are allocated in an $N \times \text{JPBLOCKS}$ array, so

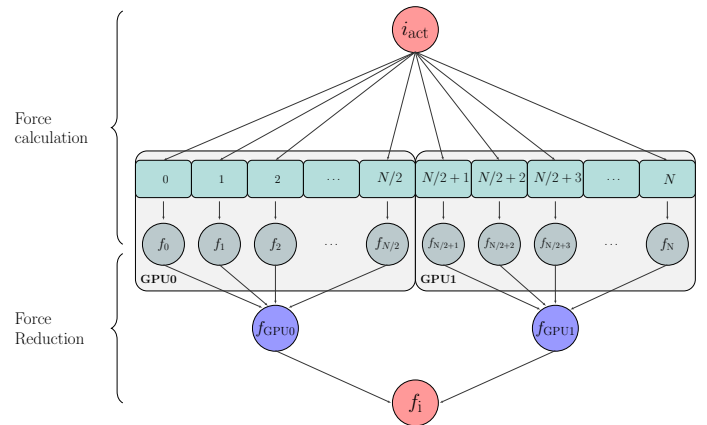


Fig. 7. parallelisation scheme to split the j -loop instead of the i -loop. Two GPUs are depicted to represent how the code works with multiple devices. In this case, we have two sections, the first is to calculate the force interactions of the i -particle with the whole system but by different threads (upper part). Then a reduction, per device, is necessary to get the new value for the i -particle force (f_i).

that for every particle we continuously save their force interaction with the other particles of the system. We then perform reductions (summations) to obtain the final forces for every N_{act} particle, which are distributed in JPBLOCKS (16) blocks. Hence, the kernel configuration must be different, and we use a simple one. In this case, we use a simple parallel CUDA reduction of N_{act} arrays of JPBLOCK (16) elements.

```
1 dim3 blockSize(JPBLOCKS, 1, 1); // (16, 1, 1)
2 dim3 gridSize(Nact, 1, 1); // (300, 1, 1)
```

3. The three flavours of GRAVIDY: Tests

Thanks to the fact that there is a number of codes implementing similar approaches to ours, we are in the position of running exhaustive tests on GRAVIDY. Indeed, the global dynamics of a dense stellar system (typically an open cluster, because of the limitation in the number of particles we can integrate) has been addressed numerically by a large number of authors in the field of stellar dynamics. Therefore, we have decided to focus on the dynamical evolution of a globular cluster with a single stellar population. We present in this section a number of tests to measure the performance and the accuracy of the three versions of GRAVIDY which we present using different amount of particles. Our goal is to be able to offer an OpenSource code that fits different needs and requirements. This is why this first release of GRAVIDY offers three different choices, which are general enough for different users with different hardware configurations. These are:

- The CPU version** consists in the more basic implementation in this work, a CPU version. I.e. This version uses OpenMP and is intended for a system without graphic processing units, but with many cores. This flavour can be used for debugging purposes by disabling the OpenMP directives (`#pragma omp`). This is the basis for our further development of the code.
- The MPI version** is virtually the same serial implementation, but with OpenMPI directives added to improve the performance of the hot-spots of the algorithm, in particular the

System A		datura (165 nodes)
CPU	Intel(R) Xeon(R) CPU X5650 @ 2.67GHz (24 cores)	
GPU		none
RAM		24 GB
OS		Scientific Linux 6.0
System B		gpu-01 (1 node)
CPU	Intel(R) Xeon(R) CPU E5504 @ 2.00GHz (4 cores)	
GPU	4 x Tesla M2050 @ 575 Mhz (448 cores)	
RAM		24 GB
OS		Scientific Linux 6.0
System C		krakatoa (1 node)
CPU	AMD Opteron 6386SE @ 2.8 GHz (32 cores)	
GPU	2 x Tesla K20c @ 706 MHz (2496 cores)	
RAM		256 GB
OS		Debian GNU/Linux 8
System D		sthelens (1 node)
CPU	Intel(R) Xeon(R) CPU E5-2697v2 (IvyBridge) @ 2.7GHz (24 cores)	
GPU	2 x Tesla C2050 / C2070 @ 1.15 Ghz (448 cores)	
RAM		256 GB
OS		Debian GNU/Linux 8

Table 1. Specification of the different systems of the Albert Einstein Institute used for the tests.

force and energy calculation. In this case we use the MPI library, and hence it can be run on a single machine using a certain amount of cores as “slave” processes or on a large cluster with separated machines as slaves.

- (iii) **The GPU version** discards all CPU usage and only relies on the GPU to integrate all gravitational interactions. As we mention later, we tried to use CPU combined with GPU, but we did not see any benefit in it, and the approach was hence neglected. We use CUDA to be able to interact with NVIDIA graphics processing units. The code is designed to detect the amount of present GPUs and use all of them, unless otherwise required by the user. This means that this version can use in a parallel way as many GPU cards as the host computer can harbour in a very simple and efficient way. The communication between the different GPU cards in the host computer is internal and run through Peripheral Component Interconnect Express (PCIe), a high-speed serial computer expansion bus standard, so that the data flows rapidly because of the low overhead.

The specifications of the hardware (CPU, GPU and available RAM) and operating systems we used are summarised in table 1.

3.1. Initial conditions and N -body units

For all of our tests we choose an equal-mass Plummer sphere (Plummer 1911) for the sake of comparison with other codes. We choose standard N -body units for the calculations and in the resulting output (Hénon 1971; Heggie & Mathieu 1986). This means that

- The total mass of the system is 1: $\sum_{i=0}^N m_i = 1$.
- The gravitational constant (G) is set to 1: $G = 1$.
- The total energy of the system is equal to -0.25 : $E_{\text{tot}} = K + U = -0.25$, with K and U the total kinetic and potential energy of the system, respectively.

3.2. Accuracy, performance and speed

For GRAVIDY, as we have seen, we have chosen a Hermite 4th-order integrator. The numerical error introduced scales hence as

$O(\Delta t^4)$ assuming a shared timestep, which means that the previous is true *only* if all particles are updated at every integration step. Since we use a block time step scheme, certain groups of particles share a timestep value, but not all of them. Thanks to this approach, the numerical error which we reach in our integrations is slightly less than the value mentioned previously.

Nitadori & Makino (2008) use a 6th- and 8th-order Hermite integrator scheme, which leads to higher-order (2nd and 3rd) acceleration derivatives and hence to better results in energy conservation, in particular the 8th-order case, but also in parallelisation efficiency. The reason for this is that by going to higher order in the truncation, we allow particles to populate ranges of timesteps forbidden in the lower-order approximation. This leads to a larger number of block steps, and hence more parallelism efficiency. This efficiency comes from the amount of particles updated in every block step, because using this higher order integrator, we have bigger groups of particles in every block. One of our goals for the future version of our code is to try different integration schemes, like the Hermite 6th-order scheme described before. However, for the current purpose of GRAVIDY with softening, as presented in this work, we deem it sufficient to employ a 4th-order, which yields a good conservation of the energy, as we will see below. Although GRAVIDY aims at users with access to a handful of GPU cards on one node, we note that the work of Capuzzo-Dolcetta et al. (2013), which is based on the same integrator, shows a good performance in large GPU clusters, which means that theoretically one could run the current version of GRAVIDY in this kind of facility.

We have introduced in Eq. (21) a free parameter, η , responsible for determining the calculation of every timestep of the system, from the initial calculation to the update after every iteration. Hence, so as to assess an optimal value for it, we perform different tests to find a balance between a good energy conservation and a minimum clock execution time. We explore values between 0.001 and 0.1 integrating a series of systems with N ranging between 1024 to 32768, for convenience¹⁴, and up to 2 NBU. We show the results in Fig.(8) performed on System B of Tab. (1). For small values of η , the cumulative energy error approximately stays constant, because the error is small enough to leave accuracy in hands of the integrator scheme and the hardware. Increasing η leads to larger errors. This is particularly evident when we use systems with a larger number of particles. The system with $N = 32768$ particles, and a $\epsilon = 10^{-4}$, achieves $\Delta E/E_0 \approx 10^{-3}$ for $\eta = 0.1$, while it is as low as $\Delta E/E_0 \approx 10^{-6}$ for the same value and 1024 particles.

In the same figure we describe the performance in function of η by using the clock time in seconds for the code to reach one NBU for the same values of the parameter. We can see that the value of η is inversely proportional to the time, since increasing its value results in decreasing the execution time. When we increase η we implicitly increase the timestep of every particle, so that one unit of time is reached sooner. We find that a value of about 0.01 is the best compromise for most of our purposes, yielding an accuracy of about $\Delta E/E_0 = 10^{-7}$ in most of the cases.

To measure the execution speed of our code we perform a set of tests by integrating the evolution for one NBU of a Plummer sphere with different particle numbers, ranging from $N = 1024$ to $N = 262144$. For the analysis, we choose the time starting at $t = 2$ and finishing at $t = 3$, since the first time unit is not representative because the system can have some spurious numerical

¹⁴ Any number of particles can be also handle properly, not necessarily powers of 2.

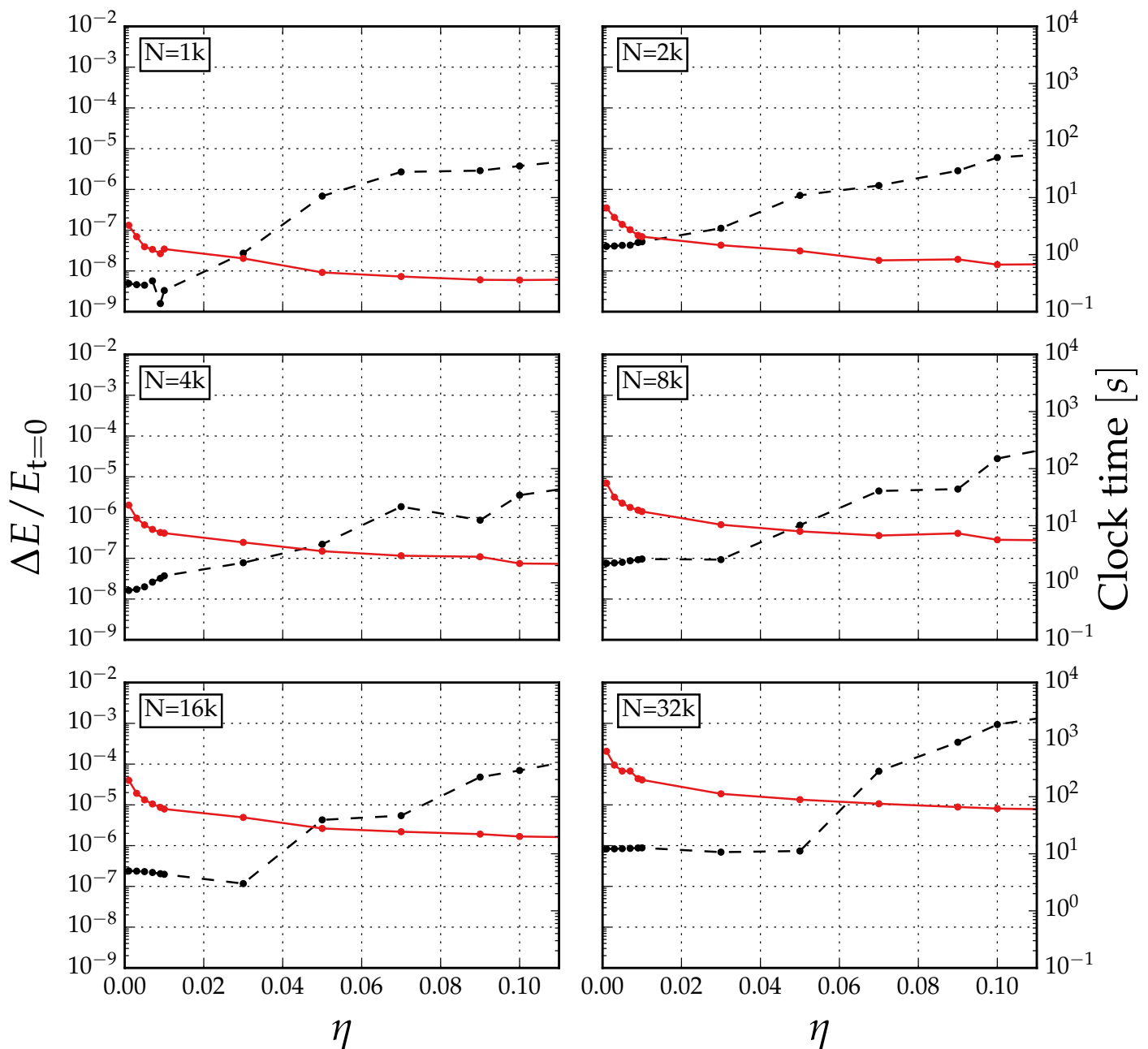


Fig. 8. Cumulative energy error (dashed black line) and wall clock time (solid red line) in function of η for six different systems consisting of a Plummer sphere with $N = 1, 2, 4, 8, 16, 32$ k particles, with $k := 1000$, from the top to the bottom, left to right. The integration corresponds to one time unit, namely from $t = 1$ to $t = 2$ in the wall clock time analysis, and for $t = 2$ in the energy error calculation. The reason for choosing the elapse between 1 and 2 is to get rid of any initial numerical error at the simulation startup, from 0 to 1. All tests have been performed on System B of Tab. (1).

behaviour resulting from the fact that it is not *slightly* relaxed. When testing the parameters η and ϵ , we picked the time starting at $t = 1$ and finishing at $t = 2$ because we wanted to understand their impact right at the beginning of the simulation. Now we allow the system to further relax so as to obtain a more realistic system. In particular, the distribution timesteps drifts away from the initial Gaussian setup. For the simulations we choose $\eta = 0.01$ and $\epsilon = 10^{-4}$ which, as we discussed previously, are a good compromise in terms of accuracy and performance.

We display the wall clock time of each integration in Fig. (9). We also display reference curves for the powers of N^3 , N^2 and $N \log N$, multiplied by different factors to adapt them to the fig-

ure. We see that GRAVIDY scales very closely as a power of 2. The deviations arise from the fact that not all particles are being updated at every timestep.

We employ different combinations of techniques during the parallelisation, both at GPU and CPU level. One of the most important points in the development of the algorithm is the low amount of work required by the GPU when $N_{\text{act}} \ll N$, as we have seen. To address this we have explored other algorithms, such as using only the CPU when $N_{\text{act}} \propto N$, with α a free parameter to be determined by the experiment of interest, or when $N_{\text{act}} < N_{\beta}$, with N_{β} a (a priori) fixed amount of particles. In both cases, none

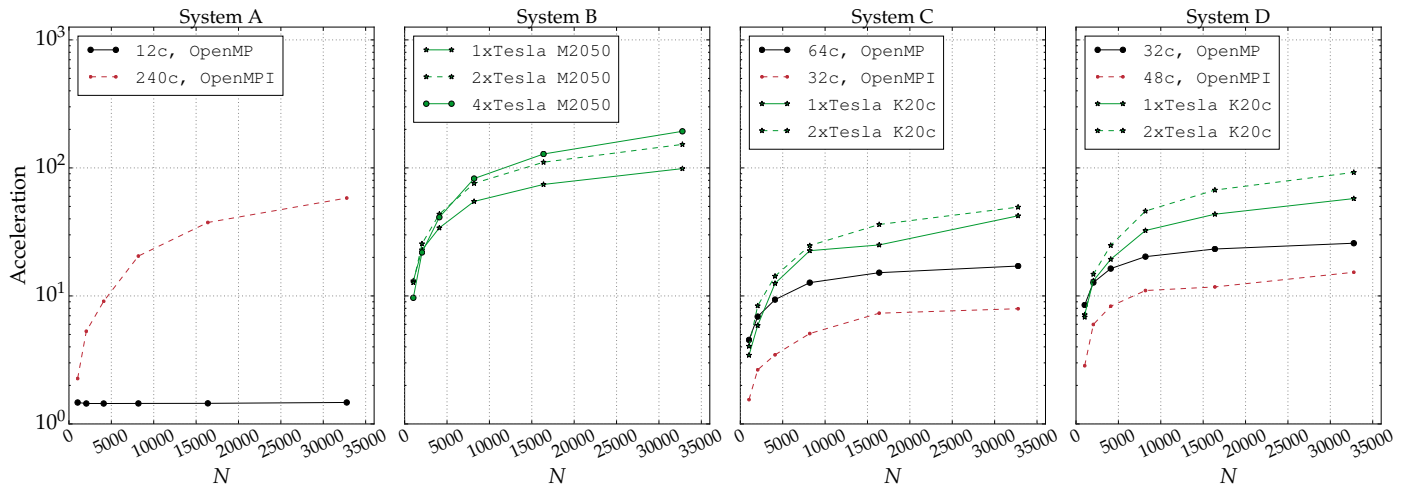


Fig. 10. Acceleration factor for the different parallel versions of the integrator, (see Tab. 1) normalised to the single-thread CPU version, up to $T = 3[NBU]$. For the CPU parallel version of the code, we give information about the number of cores with the letter “c”. The GPU-parallel cases display the information on the number of cards with multiplying numbers.

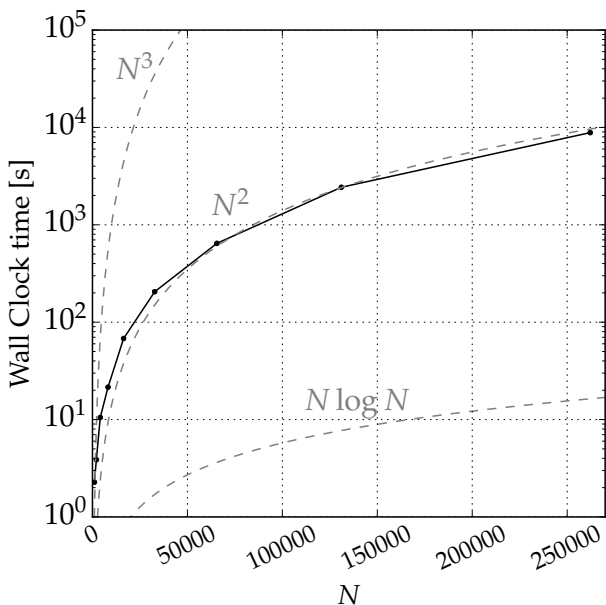


Fig. 9. Wall clock time of integration from $t = 1$ NBU up to $t = 2$ NBU, using $\eta = 0.01$ and $\epsilon = 10^{-4}$ using different amount of particles on System C of Tab.(1).

turned out to be better than the j -parallelisation, even with very small amount of N_{act} , because of the prevailing GPU usage.

In Figure 10 we show the acceleration factor for all parallel scenarios as compared to the single-thread CPU case, which we use as a reference point. Due to the design of the code, the maximum performance is achieved with the larger particle number. The most favourable scenario for GRAVIDY is, as we can see in the figure, System B. The 4 GPUs available boost the performance up to a factor of 193 as compared with the single-thread CPU case. A similar speed up is achieved on System D, which reaches a factor of 92 for the 2 GPUs. The CPU-parallel version lies behind this performance: only reaching a factor of 58 for System A, using up to 240 cores.

3.3. Scaling of the three different flavours of the code

An obvious question to any user of a numerical tool is that of scaling. In this subsection we present our results for the three different versions of GRAVIDY of how wall clock time scales as a function of threads or cores, or what is the acceleration of the multiple-GPU version of the code in function of the particle number as compared with a single GPU run, which we use as reference point.

In Fig. (11) we depict this information for the CPU, MPI and GPU versions. We can see in the CPU version that for small amounts of particles, in particular for 2k and 1k, we have an increase in the execution time with more threads, contrary to what we would expect. This is so because the amount of parallelism is not enough and the code spends more time splitting data and synchronising threads than performing the task itself, a usual situation in tasks with a low level of computation.

The MPI version uses the same j -parallelisation idea from the GPU one. In this case the code splits the whole system to the amount of available slaves (be it cores or nodes), performs the force calculation and finally sums up (“reduces”) the final forces for all active particles. This procedure is not possible with native MPI function, which is why we have developed our own forces datatype operations and reduction. The simulations with small amount of particles (1k, 2k, 4k, 8k and 16k) are a clear example of a parallelisation “overkill”: using more resources than what is actually needed. Additionally, the communication process plays a role in scaling, which can be seen in the curves corresponding to these simulations for a number larger than 200 cores - the execution time increases instead of decreasing. On the other hand, large amount of particles (cases with 32k, 64k, 128k and 256k) show the expected behaviour, a better execution time with more nodes or cores. Surely this is not a solution for all simulations, since at some point the curves flatten.

The GPU version is a different scenario, since every device has its own capability, limitations and features that makes it difficult to compare their performances. For this reason we have decided to present the acceleration factor of every case normalised to a single-GPU run in the same system. This flavour of GRAVIDY should always have a better performance when increasing the particle number. Although having a good occupancy is in principle the ideal scenario in this case, it is not necessarily the best

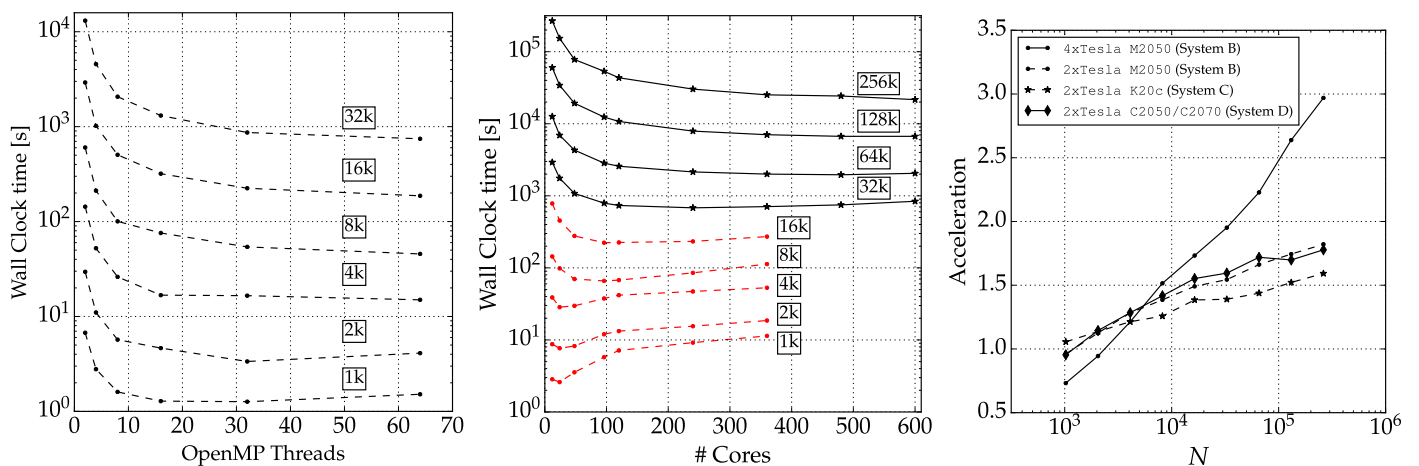


Fig. 11. Performance of the three different flavours of GRAVIDY, in function of the number of OpenMP threads, cores and GPUs, for the CPU, MPI and GPU versions, respectively and from left to right. *Left panel:* The CPU version runs on a single node with different numbers of threads. The integration corresponds to one NBU, the one from $t = 1$ to $t = 2$ to avoid spurious numerical errors from the initial setup. The experiments were performed on system C of Tab.(1). As expected, the execution time improves with the amount of threads. *Mid panel:* The MPI version running on different numbers of cores, using up to 600 of them and particles, up to 262144. In this case we use system A of the same table. Also in this case, and congruent with our expectations, using more cores leads generally to a better execution time for large amount of particles, while small systems (red lines), $< 16k$ have a poor performance. *Right panel:* The GPU flavour using different amount of devices in parallel and particles. We show the acceleration factor as compared to a single GPU run for three different setups with different GPU specifications, corresponding to systems B, C and D of the same table.

reference point to assess the efficiency of the CUDA kernels, because it is related to register uses, but also to the amount of redundant calculations and the arithmetic intensity. We show the acceleration factor of two and four Tesla M2050 devices as compared to a single-GPU run which have hardware and performance differences¹⁵ but they nonetheless reach a similar acceleration factor. We have access to two Tesla K20c, which has more than the double peak performance in double precision floating point compared to the other mentioned models. We notice a maximum factor of only 1.6 with 2 devices, which is related to the optimisation process and the scalability of the code, that was based on the M2050 model specs (the size of the block of threads we launch on every call). Every GPU is a different device, so that in order to obtain a proper optimisation we need to first do a study in terms of kernel calls configuration, which in our case is the M2050 model.

4. The role of softening on dynamics

For the current version of GRAVIDY, and quoting Sverre Aarseth on a comment he got some years ago during a talk, “we have denied ourselves the pleasure of regularisation” (Kustaanheimo & Stiefel 1965; Aarseth & Zare 1974; Aarseth 1999, 2003). This means that the code resorts to softening, via the parameter ϵ , introduced in Eq. 11. This quantity can be envisaged as a critical distance within which gravity is, for all matters, nonexistent. This obviously solves the problem of running into large numerical errors when the distance between two particles in the simulation become smaller and smaller, because since they are 0-dimensional, this induces an error which grows larger and larger as they approach. This comes at a price, however. The relaxation

time of the system is, approximately (see e.g. section on Two-body relaxation by Amaro-Seoane 2012),

$$t_{\text{rlx}} \sim N_* \frac{t_{\text{dyn}}}{\ln(d_{\text{max}}/d_{\text{min}})}. \quad (23)$$

In this equation d_{min} and d_{max} are the minimum and maximum impact parameters. In an unsoftened N -body problem they are of the order of $d_{\text{min}} \approx Gm/\sigma^2$, and the size of the cluster, respectively. In other words, $d_{\text{min}} \approx R_{\text{cl}}/N$, with R_{cl} the radius of the self-gravitating cluster, if the system is virialised, and d_{max} is of the the half-mass radius order. Now suppose the code uses a softening parameter ϵ . If the value of ϵ is smaller than d_{min} , then softening should play only a minor role in two-body relaxation, and the global dynamical evolution of the cluster must be similar to that of another cluster using regularisation. In the contrary case in which $\epsilon > d_{\text{min}}$, the relaxation time is artificially modified, as we can read from the last equation. The larger the quantity $\ln(d_{\text{max}}/d_{\text{min}})$, the more efficient is relaxation, and hence the shorter the relaxation time.

4.1. “Best” value for the softening?

We perform a series of simulations to assess the relevance of ϵ in the global dynamical evolution of an autogravitating stellar system. In Figure 12 we depict the energy error and wall clock time for six different particle numbers as a function of the softening. The lower its value, the faster the simulation. However, by using larger and larger values of the softening, we must understand that we are evolving a system in which two-body deflections, the kernel of relaxation, are not taking into account at larger and larger encounters. The fundamental feature which drives the global evolution of the system is non-existing below larger and larger distances. In particular, the larger values correspond to about 10% of the virial radius of the system. Also, the impression that energy is well conserved is artificial, so that in

¹⁵ The primary difference is that model M is designed for Original Equipment Manufacturer (OEM) for an integrated system, without active cooling, while model C includes the active cooling and can be installed on any standard computer.

some cases we obtain a good conservation (the two lower panels) or a bad one, as in the $N = 1024$ case (which, on the other hand, one should take with caution due to the very low number of particles). From these panels it seems that a value of $\epsilon \approx 10^{-4}$ is a good compromise for this particular test that we are running in this example. A good practice would be that the user tests different softening values for the case which is being addressed before making a decision for the softening. This choice is left for the user of the code, because we deem it difficult, if not impossible, to implement a self-regulating scheme in which the best value for the softening is calculated a priori.

4.2. Core collapse

4.2.1. Single-mass calculations

A good reference point to assess the global dynamical evolution of a dense stellar system is the core collapse of the system (see e.g. Spitzer 1987; Aarseth et al. 1974; Giersz & Spurzem 1994). We present here the evolution of the so-called ‘‘Lagrange radii’’ (the radii of spheres containing a certain mass fraction of the system) in Figure 13, for three representative values of the softening, the three upper panels, as calculated with GRAVIDY, and depict also the results of one calculation performed with NOBODY6GPU (Nitadori & Aarseth 2012), the lower panel, which uses KS regularisation (Kustaanheimo & Stiefel 1965; Aarseth 2003). This can be envisaged as the ‘‘best answer’’, which provides the reference point with which the other calculations should be compared. In the figures we use the half-mass relaxation time, which we introduce as

$$t_{\text{th}} = 0.138 \left(\frac{Nr_h^3}{Gm} \right)^{\frac{1}{2}} \frac{1}{\ln(\Lambda)}, \quad (24)$$

where N is the number of particles of the system, m the average mass of a star, r_h the half-mass radius, and $\Lambda := \gamma N$, with $\gamma = 0.1$ the argument of the Coulomb logarithm.

From the panels we can easily see the impact of the softening parameter in the calculations: the collapse of the core is retarded for larger values. Our default choice for the softening, 10^{-4} is just $2 T_{\text{th}}$ earlier than a NOBODY6GPU calculation that we perform to compare with our code.

Another way of looking at the core collapse is in terms of energy. In Figure 14 we display the evolution of the energy for the same systems of Figure 13. As the collapse develops, the average distance between particles becomes smaller and smaller. There is an obvious correlation between the conservation of energy and the value of the softening. The transition between a fairly good energy conservation and a bad one happens more smoothly for larger and larger values of the softening, since the error has been distributed since the beginning of the integration. This means that, the smaller the value of the softening, the more abrupt the transition between the good and bad energy conservation, which leads to a big jump for the lowest value, 10^{-5} . We stop the simulations at this point because of the impossibility of GRAVIDY to form binaries, the main way to stop the core collapse.

As discussed previously, and as we can see in Figures (14, 13), the introduction of softening in the calculations has an impact on the global dynamical behaviour of the system. We find factors of 1.001, 1.08 and 1.55 of delay to reach the core collapse for the softening values $\epsilon = 10^{-5}$, $\epsilon = 10^{-4}$ and $\epsilon = 10^{-3}$, respectively.

The NBODY6GPU simulation was run on a different system, using a GeForce GTX 750 (Tesla M10) GPU. So as to compare with GRAVIDY, we need to consider the peak performance of the GPUs in Single Precision (SP) and Double Precision (DP), as well as the number of used GPUs. NBODY6GPU uses SP, while GRAVIDY uses DP, and we estimate¹⁶ a difference in computational time to reach the core collapse of 1.88 in favour of GRAVIDY as compared to NBODY6GPU. This difference arises from the close encounter treatments of the latter.

4.2.2. Calculations with a spectrum of masses

Additionally to the single-mass calculations, we have also addressed multi-mass systems. The fact of having an Initial Mass Function (IMF) accelerates the core collapse of the system, as shown by many different authors (Inagaki & Wiyanto 1984; Spitzer 1987; Kim & Lee 1997; Kim et al. 1998). In our calculations, we use a Plummer sphere with a Kroupa IMF (Kroupa 2001) and 8192 particles. In Figure (15) we present the evolution of the Lagrange radii and the energy conservation of the system. We can see that the core collapse happens around $2 T_{\text{th}}$, which is the point from which the energy conservation becomes worse and worse, to achieve a value of about 6 orders of magnitude worse than in phases before the collapse. Another way of depicting the collapse is by identifying the heaviest 10% of the stellar population and how it distributes in the core radius as calculated at $T = 0$. We can see this in Figure (16).

The equilibrium of the system can be evaluated by analysing the distribution of the timesteps. As we have mentioned previously, in Section (2.4), the initial distribution of timesteps in the system has a Gaussian distribution, which in a balanced system must remain similar, or close. In Figure (17) we show the step distribution after the core collapse for the single-mass system with $\epsilon = 10^{-4}$

5. Conclusions and future work

In this work we have presented the first version of our new N -body code, written purely in C/C++, using OpenMPI and CUDA, which we call GRAVIDY. The current version of our code provides an environment to evolve a self-gravitating stellar system, and uses a Hermite 4th-order integration scheme, using block time steps and softening. This first release of GRAVIDY should be considered as the ‘‘poor man’s’’ multiple-GPU/CPU N -body code; i.e. we have focused on users who can have access to a machine hosting 1-2 GPU nodes, or usual parallel CPU systems.

We summarise here the main features of GRAVIDY:

1. The code is written using an iterative and incremental development, which is methodology similar to the Assess, Parallelise, Optimise, Deploy (APOD) development cycle presented by NVIDIA.
2. The code organisation is designed to be highly modular. Every critical process of the integrator is represented by a separate function or chain of functions. Our goal is to produce

¹⁶ The GTX 750 (A) has a peak performance of 1110 SP (no DP support) and we used 1 device. Our run was done on a Tesla K20c (B), of peak performance 3524 in SP and 1175 in DP, and we used 2 devices. NBODY6GPU uses SP, while GRAVIDY uses DP. A rough estimate can be done by considering A and B: $A_{SP}/B_{SP} \times 1.9 \approx 0.16$, then NBODY6GPU wall clock time (2×10^6 seconds) can be multiplied by this factor, which yields around 3.2×10^5 seconds. Our three simulations took 1.7×10^5 , 1.3×10^5 and 1.3×10^5 seconds, which gives approximately a 1.88 factor.

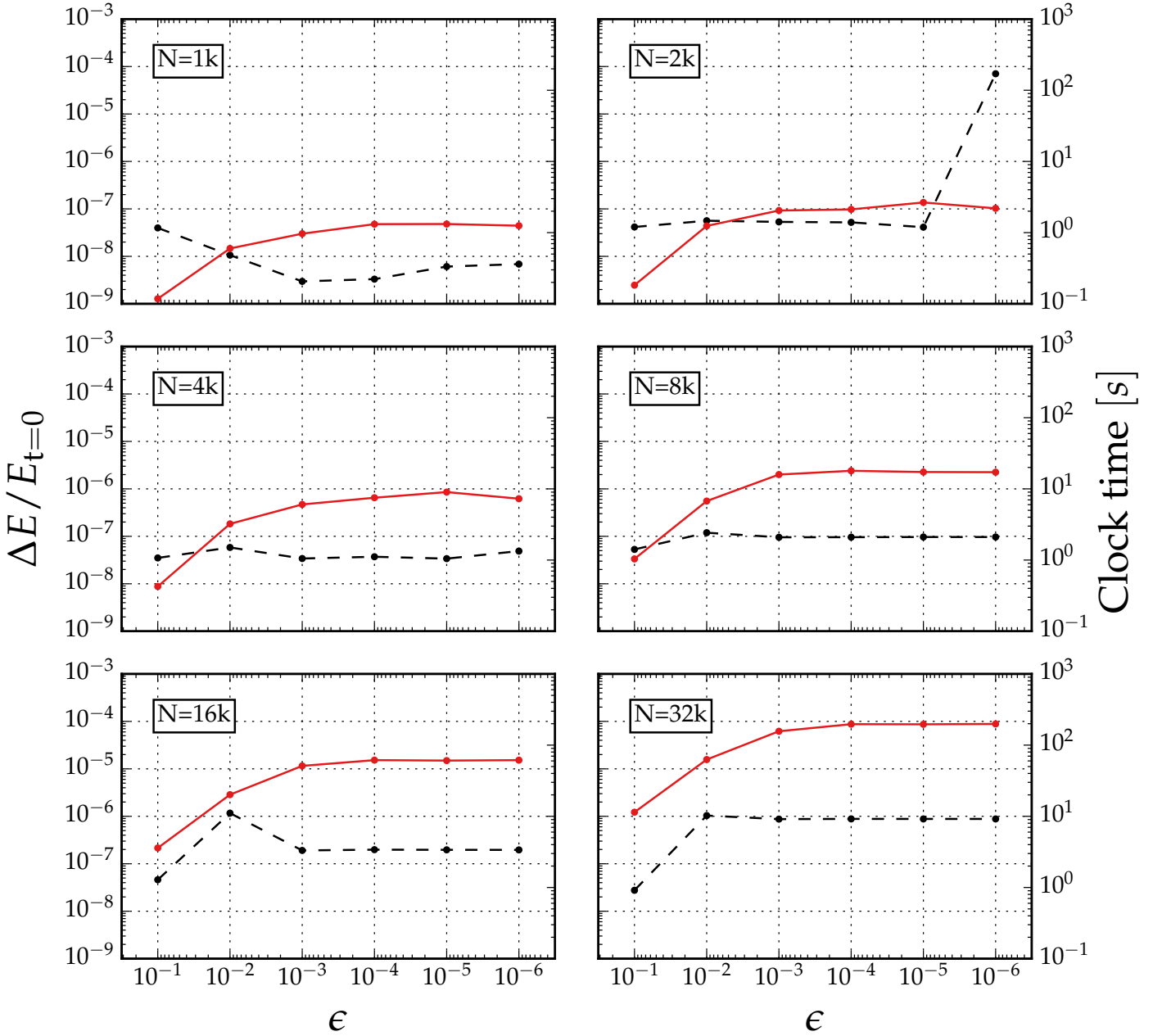


Fig. 12. Cumulative energy error (dashed black line) and wall clock time (solid red line) using different values of the softening (ϵ). We integrate different amounts of particles N up to $t = 2$ NBU. The wall clock time corresponds to the execution time between $t = 1$ and $t = 2$ NBU while the energy error is the one at $t = 2$ NBU.

a code which can be read without difficulties, which makes easier future modifications or forks.

3. Since maintainability is one of our main goals, the documentation is also a critical factor. We document every function in the inner procedure of the integrator.
4. We use a Hermite 4th order integrator scheme.
5. The code uses block time steps to improve the performance of the integrator. We evolve particles in groups of block time steps, which allows for an update of several particles at the same time.
6. We use GPU computing techniques, OpenMP and OpenMPI to parallelise the calculation of the gravitational interactions of our system after having localised the hot-spots of our algorithm. The main objective here was to be able to update a relatively small amount of particles which share a common

time step in a given moment, a situation which is against the design of GPU cards, developed to reach a high parallelism.

In this first release of GRAVIDY and first paper, we have presented a series of classical tests of the code, as well as a study of the performance of its different “flavours”: the single CPU version, the MPI one and the GPU version. We also address the role of the softening in the global evolution of a system, as integrated with our code. As expected, the value of the softening is crucial in determining the global dynamics, and should not be taken lightly, in particular if one is interested in studying physical phenomena for which relaxation is important, since using a softening translates into a maximum increase of the forces and the a smoothly declination to zero, which is approximate. To study a dynamical process, such as e.g. the collision of two

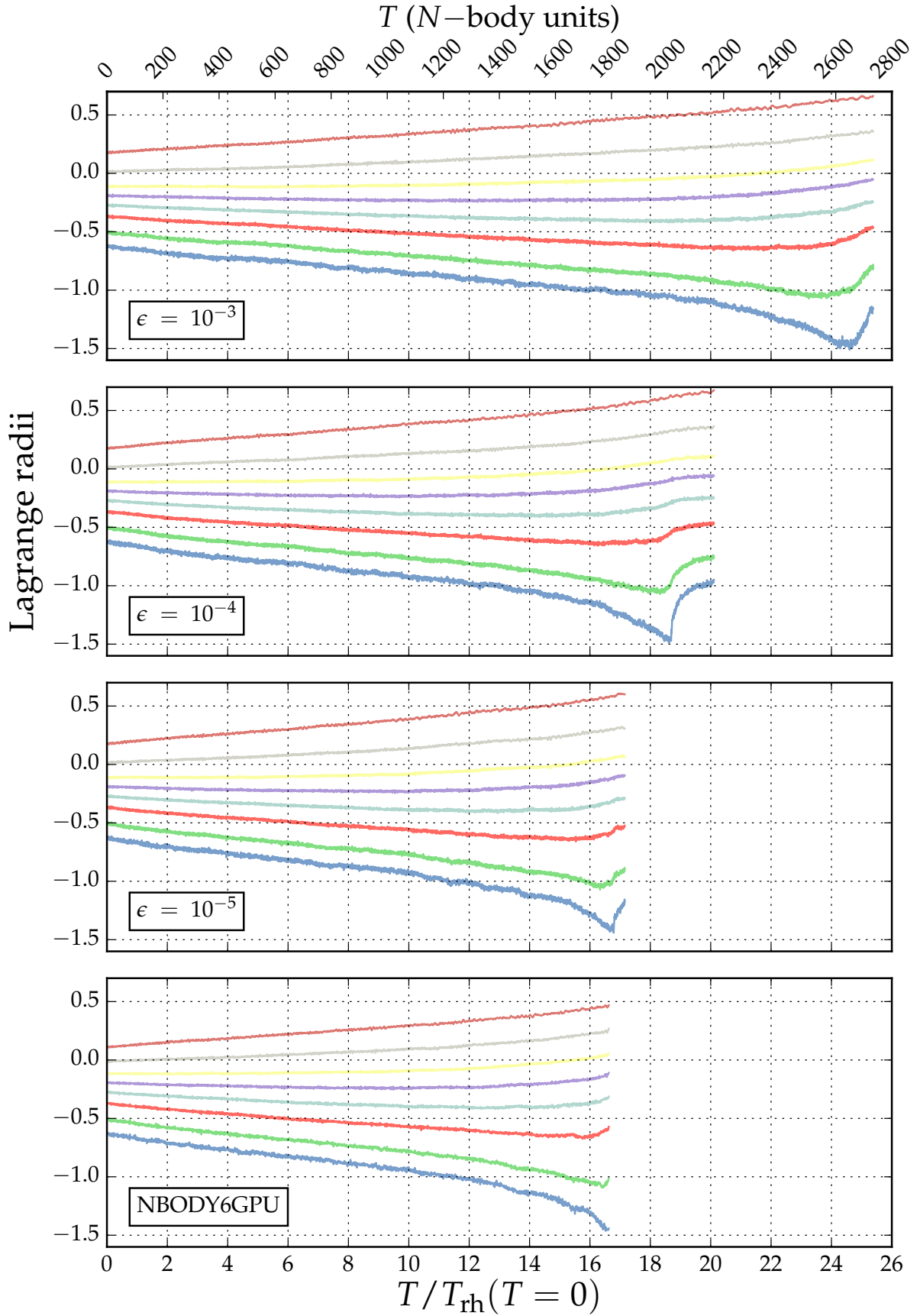


Fig. 13. Comparison of the Lagrange radii of a Plummer Sphere with $N = 8192$ particles, using different values of ϵ (softening) for GRAVITY and the NBODY6GPU code, from upper to bottom. The mass percentages are 0.5, 1, 2, 3, 4, 5, 6, 75 and 90% of the total mass, from the bottom to the upper part of each plot. The core collapse is reached at $\approx 24, 18$ and $16 T_{\text{rh}}$ for $\epsilon = 10^{-3}, 10^{-4}$ and 10^{-5} respectively. The half-mass relaxation time for this system is $T_{\text{rh}} = 112.186[NBU]$. The NBODY6GPU code does not include a softening parameter, and treat binary evolution with a KS-regularisation.

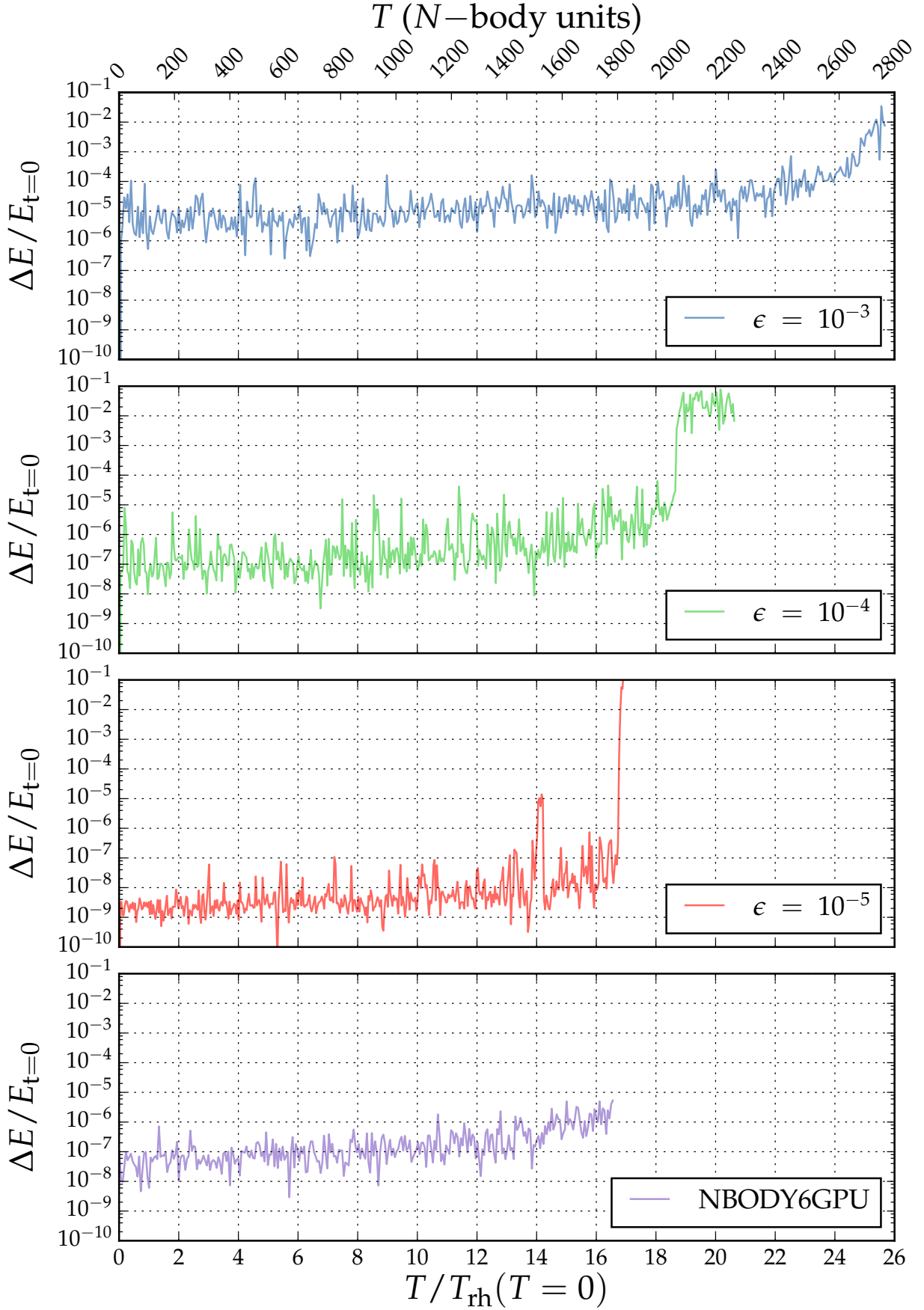


Fig. 14. Energy conservation in a long time integration of a system with $N = 8192$ Comparison of the Energy conservation of a Plummer Sphere with $N = 8192$ particles, using different values of ϵ (softening) for GraviDy and the NBODY6GPU code, from upper to bottom. The core collapse is reached at $\approx 24, 18$ and $16 T_{\text{rh}}$ for $\epsilon = 10^{-3}, 10^{-4}$ and 10^{-5} respectively. The half-mass relaxation time for this system is $T_{\text{rh}} = 112.186[NBU]$ The NBODY6GPU code does not include a softening parameter, and treat binary evolution with a KS-regularisation. All the runs were stopped after the core collapse.

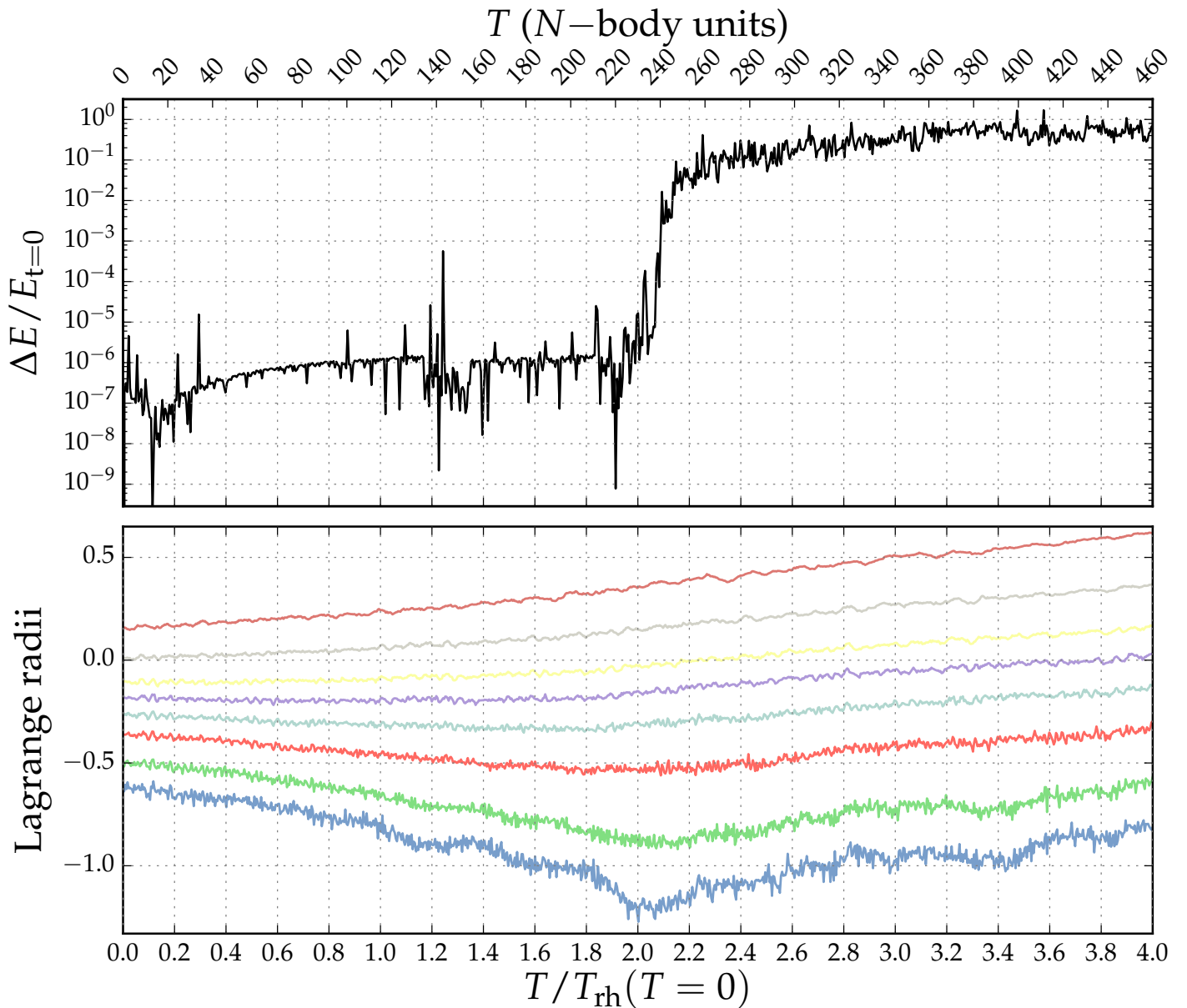


Fig. 15. Plummer sphere using 8192 particles and following a Kroupa IMF. *Top Panel:* Cumulative energy of the system. *Bottom Panel:* Lagrange radii distribution for 0.5, 1, 2, 3, 4, 5, 6, 75 and 90% of the total mass.

clusters, focusing on the short-term (i.e. for times well below a relaxation time) dynamical behaviour of the system, using a softening should be fine, but the role of the parameter should be assessed carefully by exploring different values.

The on-going development of GRAViDY includes a close encounter solver, with a time-symmetric integration scheme to treat binaries, such as the one presented in the work of (Konstantinidis & Kokkotas 2010). Another immediate goal of the next releases, is to include a central massive particle and the required corrections to the gravitational forces so as to ensure a good conservation of the energy in the system. This massive particle could be envisaged as a massive black hole in a galactic centre or a star in a protoplanetary system. We also plan on bridging the gap between spherical nucleus models that focus on collisional effects and simulations of larger structure that are able to account for complex, more realistic non-spherical geometry. Finally, a future goal is to include stellar evolution routines, from which the

modularity of our code will provide an easy scenario. One of the candidate modules for this could be SEVN (Spera et al. 2015).

We will follow the APOD cycle presented in this work, it is necessary to study new computational techniques, so as to improve the performance of our code: from variable precision to new parallel schemes to perform the force interaction calculation, using one or more GPU.

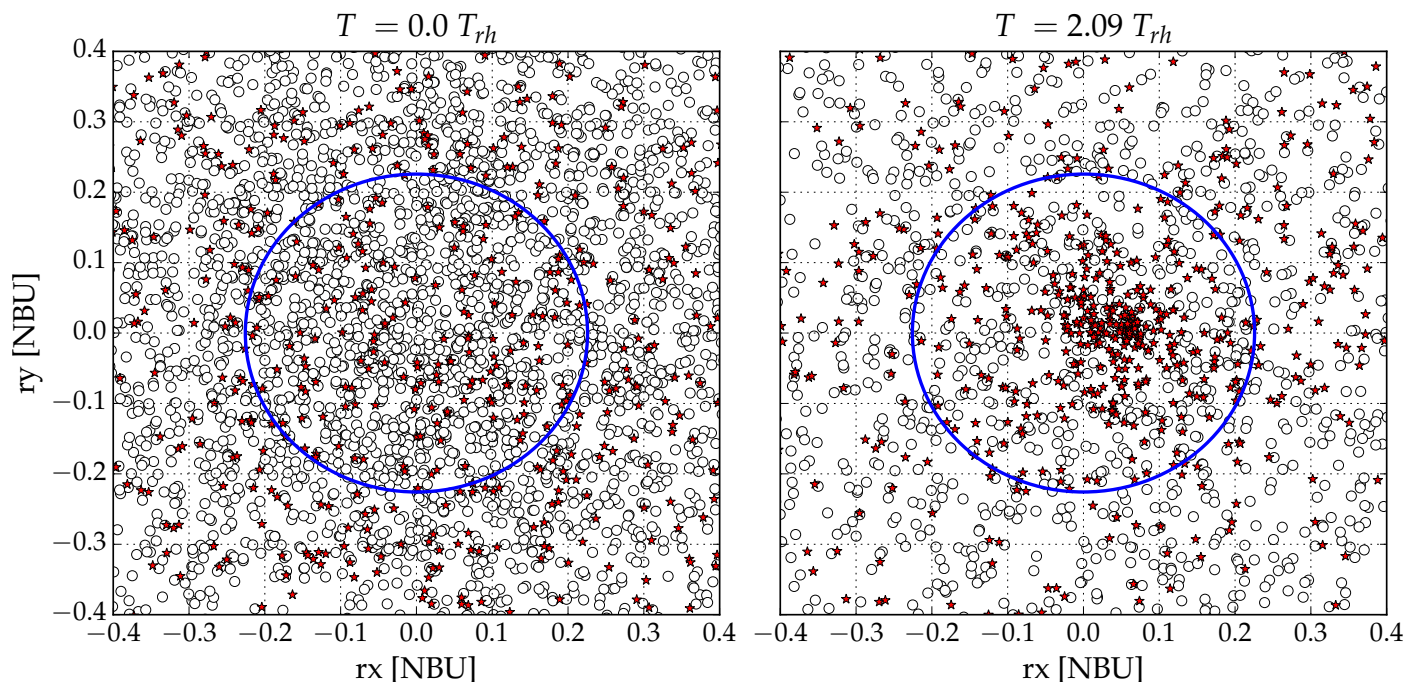


Fig. 16. Inner section of a Plummer sphere with 8192 particles Plummer sphere following a Kroupa IMF before (left) and after the core collapse (right) at $T = 2.09 T_{rh}$. The blue circle depict the core radius at $T = 0$. The top 10% of the heaviest particles in the system are marked as red stars, while all other particles as empty circles.

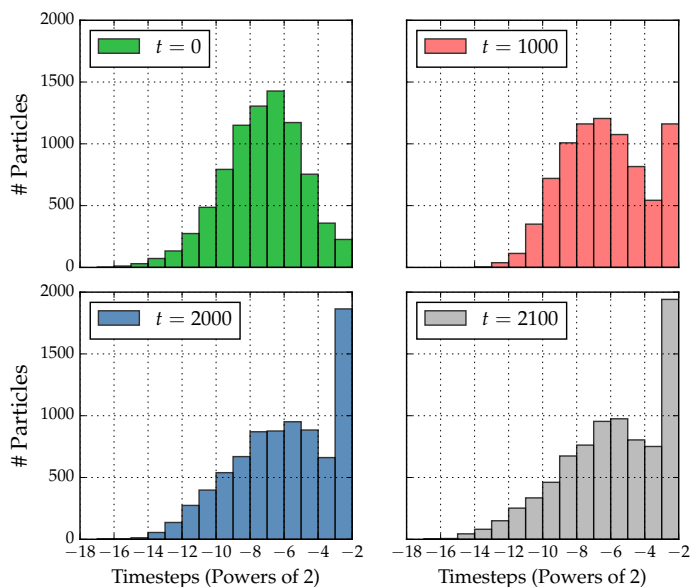


Fig. 17. Timestep distribution of a Plummer sphere with $N = 8192$ particles. Four different times are shown, (1) $t = 0$ NBU, for an initial distribution (upper left panel) (2) $t = 1000$ NBU, a few half-mass relaxation times $\sim 9 T_{rh}$ (upper right panel), (3) $t = 2000$ NBU, a pre core-collapse stage with many particles leaving the core (lower left panel), (4) $t = 2100$ NBU, a post core-collapse stage with a few particles (mostly binaries) reaching smaller timesteps (lower right panel).

Appendix A: About the code

GRAVIDY is a C/C++ and CUDA application, that uses the CUDA, OpenMPI and boost libraries.

Listing 2. Example run of the integrator. Columns, decimals, and information were modified to fit the output on this document.

```

$ ./gravity-gpu -i ../input/04-nbody-p1024_m1.in -p -t 1
[2017-01-28 01:60:56] [INFO] GPUs: 1
[2017-01-28 01:60:56] [INFO] Spl. 1024 particles in 1 GPUs
[2017-01-28 01:60:56] [INFO] GPU 0 particles: 1024
Time  Iter  Nsteps  Energy  RelE  CumE  ETime
0.000  0      0      -2.56e-01  0.00e+00  0.00e+00  3.08e-02
0.125  698   30093  -2.56e-01  2.41e-07  2.41e-07  3.84e-01
0.250  1262  61319  -2.56e-01  1.10e-07  1.30e-07  6.60e-01
0.375  1897  91571  -2.56e-01  4.19e-08  8.84e-08  9.49e-01
0.500  2530  121963 -2.56e-01  8.51e-08  3.30e-09  1.23e+00
0.625  3132  150924 -2.56e-01  2.89e-08  3.23e-08  1.52e+00
0.750  3725  180446 -2.56e-01  1.39e-08  1.83e-08  1.76e+00
0.875  4354  212425 -2.56e-01  5.23e-07  5.41e-07  2.02e+00
1.000  5160  244165 -2.56e-01  2.32e-07  3.09e-07  2.32e+00
[2017-01-28 01:60:59] [SUCCESS] Finishing...

```

As an overview, the compilation can be done with: `make <flavour>`, for the cpu, mpi and gpu versions. A simple run of the code is displayed in the Listing 2.

The URL hosting the project is:

– <http://gravityd.xyz>

where you can find the prerequisites, how to get, compile and use the code more detailed. Additionally, documentation regarding the code, input and output files is included.

Appendix B: N -body visualisation tool

A graphical representation of N -body simulations is always an attractive idea to display how the simulation was performed (Fig. B.1). Due to this reason, we decided to write an small application to have a simple 3D visualisation of GRAVIDY snapshots, based in OpenGL.

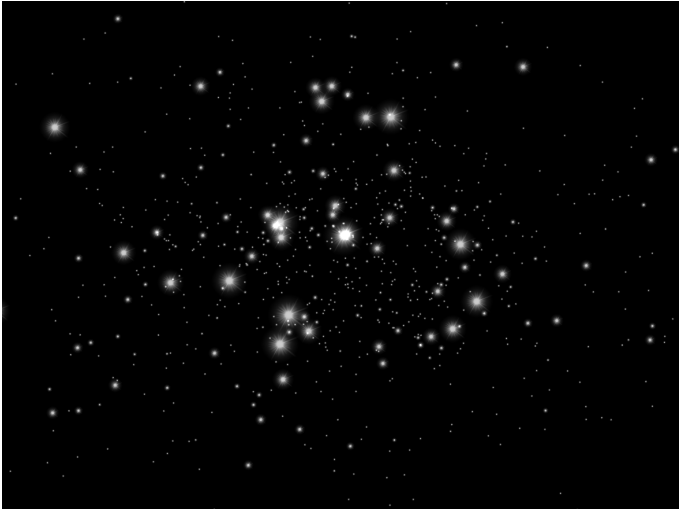


Fig. B.1. Snapshot pre-visualisation with GraviDyView using a $N = 1024$ system.

GRAVIDYVIEW is a lightweight and simple OpenGL N -body visualisation tool, written in C/C++. It can be downloaded from:

– <https://gitlab.com/cmaureir/gravidy-view>.

Acknowledgements. We are thankful for hints, help and discussion to Sverre Aarseth, Holger Baumgardt, Peter Berczik, Douglas Heggie, Piet Hut, Simos Konstantinidis, Patrick Brem, Keigo Nitadori, Ulf Löckmann and Rainer Spurzem. In general, we are indebted with the very friendly N -body community, for keeping their codes publicly available to everybody. PAS acknowledges support from the Ramón y Cajal Programme of the Ministry of Economy, Industry and Competitiveness of Spain. CMF thanks the support and guidance of Prof. Luis Salinas during the development of his Master thesis, which was the motivation of this project. This work has been supported by the “Dirección General de Investigación y Postgrado” (DGIP) by means of the “Programa Incentivo a la Iniciación Científica” (PIIC) at the Universidad Técnica Federico Santa María, the “Comisión Nacional de Investigación Científica y Tecnológica de Chile” (CONICYT) through its Master scholarships program and the Transregio 7 “Gravitational Wave Astronomy” financed by the Deutsche Forschungsgemeinschaft DFG (German Research Foundation). CMF acknowledges support from the DFG Project “Supermassive black holes, accretion discs, stellar dynamics and tidal disruptions”, awarded to PAS, and the International Max-Planck Research School.

References

- Aarseth, S. J. 1985, in Multiple time scales, p. 377 - 418, ed. J. U. Brackbill & B. I. Cohen, 377–418
- Aarseth, S. J. 1999, The Publications of the Astronomical Society of the Pacific, 111, 1333
- Aarseth, S. J. 2003, Gravitational N-Body Simulations (ISBN 0521432723. Cambridge, UK: Cambridge University Press, November 2003.)
- Aarseth, S. J., Henon, M., & Wielen, R. 1974, A&A, 37, 183
- Aarseth, S. J. & Zare, K. 1974, Celestial Mechanics, 10, 185
- Amaro-Seoane, P. 2012, ArXiv e-prints [arXiv:1205.5240]
- Amaro-Seoane, P., Freitag, M., & Spurzem, R. 2004, MNRAS [astro-ph/0401163]
- Barnes, J. & Hut, P. 1986, Nat, 324, 446
- Belleman, R. G., Bédorf, J., & Portegies Zwart, S. F. 2008, New Astronomy, 13, 103
- Berczik, P., Nitadori, K., Zhong, S., et al. 2011, 8
- Berczik, P., Spurzem, R., Wang, L., Zhong, S., & Huang, S. 2013, in Third International Conference “High Performance Computing”, HPC-UA 2013, p. 52-59, 52–59
- Capuzzo-Dolcetta, R. & Spera, M. 2013, Computer Physics Communications, 184, 2528
- Capuzzo-Dolcetta, R., Spera, M., & Punzo, D. 2013, Journal of Computational Physics, 236, 580

- Fukushige, T., Makino, J., & Kawai, A. 2005, PASJ, 57, 1009
- Gaburov, E., Harfst, S., & Zwart, S. P. 2009, New Astronomy, 14, 630
- Giersz, M. & Spurzem, R. 1994, MNRAS, 269, 241
- Greendard, L. 1987, PhD thesis, Yale University, New Haven, CT
- Hamada, T. & Itaka, T. 2007, New Astronomy [arXiv:astro-ph/0703100]
- Harfst, S., Gualandris, A., Merritt, D., & Mikkola, S. 2008, MNRAS, 389, 2
- Heggie, D. & Hut, P. 2003, The Gravitational Million-Body Problem: A Multidisciplinary Approach to Star Cluster Dynamics, by Douglas Heggie and Piet Hut. Cambridge University Press, 2003, 372 pp., ed. Heggie, D. & Hut, P.
- Heggie, D. C. & Mathieu, R. D. 1986, in Lecture Notes in Physics, Berlin Springer Verlag, Vol. 267, The Use of Supercomputers in Stellar Dynamics, ed. P. Hut & S. L. W. McMillan, 233
- Hénon, M. H. 1971, A&AS, 14, 151
- Holmberg, E. 1941, ApJ, 94, 385
- Hut, P. 2003, in IAU Symposium, Vol. 208, Astrophysical Supercomputing using Particle Simulations, ed. J. Makino & P. Hut, 331
- Inagaki, S. & Wiyanto, P. 1984, PASJ, 36, 391
- Kim, S. S. & Lee, H. M. 1997, Journal of Korean Astronomical Society, 30, 115
- Kim, S. S., Lee, H. M., & Goodman, J. 1998, ApJ, 495, 786
- Konstantinidis, S. & Korkotas, K. D. 2010, A&A, 522, A70
- Kroupa, P. 2001, MNRAS, 322, 231
- Kustaanheimo, P. E. & Stiefel, E. L. 1965, J. Reine Angew. Math., 218, 204
- Makino, J. 1991, ApJ, 369, 200
- Makino, J. 1998, Highlights in Astronomy, 11, 597
- Makino, J. & Aarseth, S. J. 1992, PASJ, 44, 141
- Makino, J. & Taiji, M. 1998, Scientific simulations with special-purpose computers : The GRAPE systems (Scientific simulations with special-purpose computers : The GRAPE systems /by Junichiro Makino & Makoto Taiji. Chichester ; Toronto : John Wiley & Sons, c1998.)
- Nguyen, H. 2007, Gpu gems 3, 1st edn. (Addison-Wesley Professional)
- Nitadori, K. 2009, PhD thesis, University of Tokyo
- Nitadori, K. & Aarseth, S. J. 2012, MNRAS, 424, 545
- Nitadori, K. & Makino, J. 2008, na, 13, 498
- Plummer, H. C. 1911, MNRAS, 71, 460
- Portegies Zwart, S. F., Belleman, R. G., & Geldof, P. M. 2007, New Astronomy, 12, 641
- Portegies Zwart, S. F., McMillan, S. L. W., Hut, P., & Makino, J. 2001a, MNRAS, 321, 199
- Portegies Zwart, S. F., McMillan, S. L. W., Hut, P., & Makino, J. 2001b, MNRAS, 321, 199
- Press, W. H. 1986, in The Use of Supercomputers in Stellar Dynamics, ed. P. Hut & S. L. W. McMillan (Springer-Verlag), 184
- Schneider, J., Amaro-Seoane, P., & Spurzem, R. 2011, MNRAS, 410, 432
- Spera, M., Mapelli, M., & Bressan, A. 2015, MNRAS, 451, 4086
- Spitzer, L. 1987, Dynamical evolution of globular clusters (Princeton, NJ, Princeton University Press, 1987, 191 p.)
- Spitzer, L. J. & Hart, M. H. 1971, ApJ, 166, 483
- Spurzem, R. 1999, Journal of Computational and Applied Mathematics, 109, 407
- Taiji, M., Makino, J., Fukushige, T., Ebisuzaki, T., & Sugimoto, D. 1996, in IAU Symp. 174: Dynamical Evolution of Star Clusters: Confrontation of Theory and Observations, ed. P. Hut & J. Makino, 141
- von Hoerner, S. 1960, Z. Astrophys., 50, 184
- von Hoerner, S. 1963, Z. Astrophys., 57, 47
- Wang, L., Spurzem, R., Aarseth, S., et al. 2016, mn, 458, 1450
- Wang, L., Spurzem, R., Aarseth, S., et al. 2015, mn, 450, 4070